

國立臺灣大學分子細胞生物所

博士論文

Institute of Molecular and Cellular Biology

National Taiwan University

PhD Thesis

線蟲 *dpy-24* 基因整合在 DTC 細胞遷移過程中

時間與空間的訊息調控

Caenorhabditis elegans dpy-24 integrates the temporal

and spatial signals to control DTC migration

黃才芳

Tsai-Fang Huang

指導教授：吳益群 博士

Advisor: Yi-Chun Wu, Ph.D.

中華民國 98 年 7 月

July, 2009

致謝

自從進入實驗室以來，此後每一天沒有一天不受到吳老師的影響，老師對於科學的態度、對於實驗的要求，既認真嚴謹又大膽求新，從沒有停止追求進步。我感謝命運讓吳老師成為我的啟蒙者，在耳濡目染之下，領受老師對於研究的態度；我感謝老師對我的期待，因著這份期待，我做得更好；我感謝老師對我的要求與訓練，讓我在科學的路上，成為更成熟的研究者。

在 *dpy-24* 的研究過程中，我有幸可以跟峻逸合作，即使日後分道揚鑣，也會記得我們在 bench 上針鋒相對的腦力激盪，記得合作無間的依存關係，謝謝峻逸這個好伙伴。感謝 814 實驗室中所有的同學，每一個人獨特的個性，讓實驗室既有趣又充滿了溫暖，也感謝大小事通包的惠雯，沒有你的幹練與負責，就難有實驗室怡人的工作環境。

我感謝我的家人，讓我有最自由的空間飛翔，小心翼翼地端著我在實驗上所有的高低潮情緒，有了你們的支持，漫漫研究路上，我能走得更穩。感謝遠在英國的妍希，我們一起分享研究路上的喜怒哀樂，雖然鞭長莫及，沒辦法給彼此擁抱，但其中濃郁的友誼，已馨香滿懷。

最後，如果我有一丁點的成就，我把它獻給我的摯愛—惟德，感謝你一直守護著我，感謝你給我一個快樂的家、一個遮風避雨的港口、一個亂發脾氣的胸口，你是上天賜給我最美好的禮物。

中文摘要

細胞遷移在生物發育過程中扮演著重要的角色，細胞在什麼時間遷移到哪個地點，都必須經過嚴格的控制；現階段對細胞遷移的研究，僅針對時間或空間調控的個別探討，而整合兩者調控的相關機制目前瞭解得很少。在雌雄同體的線蟲個體中，有兩顆 DTC 細胞在特定的發育時期會進行特定的遷移路徑，這樣的遷移路徑也決定日後生殖腺的形狀。在 DTC 爬行過程中，荷爾蒙接收器 DAF-12、Fox 蛋白質 DRE-1 及轉錄調控子 LIN-29 負責共同調控 DTC 在三齡幼蟲時期的遷移，其中包含了 DTC 從腹側到背側的背向遷移；此背向遷移需要 DTC 細胞表現 UNC-5 接收器，只要 DTC 表現 UNC-5 接收器，DTC 便會接收到位在腹側 Netrin 蛋白質的排斥訊息，而遷移到線蟲的背側。在本研究中，我們分析 *dpy-24* 突變株、研究 *dpy-24* 基因，發現 *dpy-24* 能藉由整合三齡幼蟲發育時期的時間訊息及 UNC-5 腹側排斥的空間訊息，來調控 DTC 的背向遷移；當 *dpy-24* 發生突變時，DTC 背向遷移會提早發生，而當 *dpy-24* 過度表現時，DTC 的背向遷移則會延遲發生。DPY-24 是一個具有 zinc fingers 的蛋白質，和哺乳類的轉錄抑制子 Blimp-1 和 PRDI-BF1 非常相似。藉由對 *unc-5* 轉錄表現的觀察，我們發現 *dpy-24* 會抑制 *unc-5* 的轉錄來阻止 DTC 提早進行背向遷移，之後免疫染色的結果顯現 DPY-24 在 DTC 中僅表現在 DTC 進行背向遷移之前，當 DTC 開始進行背向遷移後，DPY-24 的表現便消失了。我們發現 *dre-1*、*daf-12* 與 *lin-29* 共同負責 DPY-24 在三齡幼蟲時期的削減，DPY-24 在二齡幼蟲時期表現量最高，因此才能阻止 DTC 在不正確時間的背向遷移；而三齡幼蟲時期的時間訊息讓 DPY-24 消失，於是 DPY-24 不再抑制 *unc-5* 的轉錄，再加上此時 LIN-29 和 DAF-12 對於 *unc-5* 的活化，使得 *unc-5* 得以開始表現，在 UNC-5 順利表現後，DTC 才能進行背向遷移。

這個研究成果提供了一個在發育過程中，藉由整合時間與空間的訊息來調控特定細胞遷移的分子機制。

關鍵字：線蟲、細胞遷移、時間調控、異時基因、*dpy-24*



Abstract

Cell migration plays a key role in animal development and must be temporally and spatially regulated. However, little is known about how temporal and directional signals are integrated to give rise to specific cell migration patterns. In the *C. elegans* hermaphrodite, two somatic distal tip cells (DTC) undergo a developmental stage- and direction-specific migration pattern which determines the shape of the gonad. The heterochronic genes *daf-12*, *dre-1* and *lin-29*, encoding steroid hormone receptor, F-box protein, and zinc finger transcription factor, respectively, act together to control the third larval (L3) developmental program of the gonad, including the ventral-to-dorsal migration of the DTCs. The guidance receptor *unc-5* is both necessary and sufficient for dorsal migration of the DTCs away from the ventrally concentrated extracellular cue netrin. Here, we identify and characterize *dpy-24* mutants and show that *dpy-24* links the L3 temporal signal to the spatial regulator *unc-5* and thereby controls the timing of DTC dorsal migration. Mutations in *dpy-24* results in precocious dorsalward turning of the DTCs, whereas constitutive expression of *dpy-24* leads to retarded DTC dorsal turn. *dpy-24* encodes a zinc-finger-containing protein, similar to mammalian transcription repressors Blimp-1 and PRDI-BF1. Using an *unc-5* transcriptional *gfp* reporter, we show that *dpy-24* prevents the DTCs from precocious dorsal turn by transcriptional repression of *unc-5*. The immunostaining data reveals that DPY-24 is present in the DTCs prior to their dorsalward turning and disappears during and after the dorsal turn. Further studies indicate that *dre-1*, *daf-12* and *lin-29* are responsible for DPY-24 down-regulation at the L3 stage. DPY-24 protein level is high in L2 and thus prevents DTC from dorsalward turning. The timely disappearance of DPY-24, which is regulated by L3-specific temporal signal, leads to concomitant *unc-5* transcriptional up-regulation, likely mediated through

transcription activities of LIN-29 and DAF-12, hence allowing DTC migration to switch towards the dorsal direction. These results provide a molecular mechanism by which temporal and spatial signals are integrated to control the precise cell migration pattern during development.

Key words: cell migration, temporal regulation, distal tip cell (DTC), heterochronic, *dpy-24*, *unc-5*, *daf-12*, *dre-1*, *lin-29*



Table of Contents

致謝.....	i
中文摘要	ii
Abstract	iv
Introduction	1
Cell migration is important in development	1
DTCs provide a paradigm to study the spatiotemporal control of cell migration in <i>C.elegans</i>	2
Genes affecting DTC motility and polarity.....	3
The guidance control of DTC migration.....	4
The temporal control of DTC migration.....	6
Material and Methods	8
Strains and Genetics.....	8
EMS mutagenesis	8
<i>dpy-24</i> cloning and cDNA construction.....	9
Transgenic strains	9
Antibodies and Immunostaining	10
RNA interference	11
Yeast assay	11
Results	13
<i>dpy-24</i> mutants are defective in DTC migration.....	13
<i>dpy-24</i> mutants have a precocious DTC dorsal turn at the early L3 stage	14
DPY-24 encodes a protein with a PR domain and five zinc fingers related to the mammalian protein Blimp-1 and PRDI/BF1	15
DPY-24 is transiently present in DTCs before dorsal turn but absent after dorsal	

turn.	17
Constitutive expression of <i>dpy-24</i> delays dorsal phase II migration	17
The precocious dorsal turn of <i>dpy-24</i> mutants requires canonical Netrin/Unc-5 pathway.	18
<i>dpy-24</i> represses <i>unc-5</i> transcription to prevent precocious dorsal turn of DTCs. 19	
The zinc fingers of DPY-24 bind directly to the <i>unc-5</i> promoter at D1 and D2 sties.	21
It is difficult to reveal the biological significance of D1 and D2.....	22
Down-regulation of DPY-24 is controlled by the heterochronic genes <i>dre-1</i> , <i>daf-12</i> and <i>lin-29</i>	24
DAF-12 activates <i>unc-5</i> transcription.....	25
LIN-29 activates <i>unc-5</i> transcription.....	26
DPY-24 transcriptionally represses <i>lin-29</i> in phase I DTC migration	27
Discussion	29
A functional link between a transcription factor and a guidance receptor.....	29
<i>dpy-24</i> is a heterochronic gene	29
Transcriptional control of <i>unc-5</i>	31
<i>dpy-24</i> likely acts in parallel to <i>unc-5</i> to control the direction of the centripetal phase III migration of DTCs.....	32
Multiple regions of DPY-24 are important for DTC migration	33
DPY-24 down-regulation is controlled by heterochronic genes <i>daf-12</i> , <i>dre-1</i> and <i>lin-29</i> to initiate the dorsalward turning of DTCs.....	34
<i>lin-42</i> might play as a switch for DTCs making dorsal turns or not.....	35
UNC5B might be the target of Blimp-1 during lymphocyte chemostasis.....	36
Evolutionary conservation of DPY-24 and Blimp-1 genes in the control of cell	

identities during development.....	36
Reference	38
Figures and Tables	48
Figure 1. DTC migration defects in <i>dpy-24</i> mutants.	48
Figure 2. <i>dpy-24</i> mutant exhibits white patches under dissecting microscope.....	49
Figure 3. The migration speed of DTC in <i>dpy-24</i> mutant is similar to that in N2 wild type.....	50
Figure 4. DTC makes a precocious dorsal turn in <i>dpy-24</i> mutant.	52
Figure 5. DTC makes its dorsal turn 3.5 hr earlier in <i>dpy-24</i> mutant than in N2 wild type.....	53
Figure 6. The genetic mapping and molecular cloning of <i>dpy-24</i>	54
Figure 7. The <i>dpy-24</i> gene and protein.....	55
Figure 8. Dpy-24 expression pattern.....	56
Figure 9. DPY-24 expression is transient in the first phase of DTC migration and its expression is complementary to <i>unc-5</i> expression.....	57
Figure 10. <i>unc-5</i> is precociously activated in <i>dpy-24</i> mutant and is suppressed when <i>dpy-24</i> is ectopically expressed.	58
Figure 11. DPY-24 binds to the <i>unc-5</i> promoter <i>via</i> its zinc fingers.	60
Figure 12. DPY-24 is abnormally present in the DTCs of <i>lin-29;daf-12</i> , <i>lin-29;dre-1</i> and <i>dre-1;daf-12</i> double mutants at the L4 stage.	61
Fig 13. DAF-12 directly binds to the <i>unc-5</i> promoter.	62
Figure 14. DAF-12 itself could activate the <i>unc-5</i> promoter.	63
Figure 15. <i>unc-5</i> expression is absent in <i>lin-29;daf-12</i> double mutant.....	64
Fig 16. <i>dpy-24</i> suppresses the transcription of <i>lin-29</i> in early L2.	65
Fig 17. The model of the interaction between <i>dpy-24</i> and heterochronic genes to	

regulate the expression of *unc-5*.66

Table 1. DTC migration patterns in *dpy-24* mutants and transgenic worms67

Table 2. Genetic interactions of *dpy-24* with *unc-5*, *unc-6*, *unc-40* and *unc-129*.68

Table 3. The genetic interaction between *dpy-24* and heterochronic genes *lin-29*,
dre-1 and *daf-12* in posterior DTC migration.....69

Table 4. Ectopic expression of *lin-29* is sufficient to induce DTC dorsal turn and
unc-5 expression.70



Introduction

Cell migration is important in development.

Cell migration plays an important role in animal development (Hedgecock et al. 1987; Antebi 1997). For example, during vertebrate gastrulation extensive cell migrations occur to generate three-layered embryos. Later, the cells in the epithelium layer migrate to various locations and differentiate into specialized cell types that form different tissues and organs. In adult, cell migration is also a crucial component in life maintenance in adults. In the renewal of skin and intestine, the new epithelium cells migrate to the surface from the basal layers. When the organism is attacked by the foreign pathogen, the leukocytes migrate from the circulation into the surrounding tissue to destroy the invading enemies. On the other hand, cell migration plays an important role in metastasis, characterized by the invasion of cancerous cells. Therefore, studies of mechanisms of cell migration are of biological importance and medical relevance.

The cell migration process in general includes the following five steps. First, the cell extends the pseudopod at the leading edge. Second, the extended pseudopod is immobilized by forming a focal contact with the matrix. Third, the modification (such as proteolysis) of the surrounding extracellular matrix is required for the whole cell body to move. Fourth, the cell contracts and squeezes to the front. In the last step, the cell releases the attachment of the trailing edge and moves forward. In developing organisms, cell migration is regulated by spatial and temporal signals. Many guidance molecules, such as netrin, semaphorin, Ephrin, Sonic hedgehog, Wnt and Robo etc, and their respective receptors and signaling pathways have been extensively studied (Hirai et al. 1987; Hedgecock et al. 1990b; Rothberg et al. 1990; Ishii et al. 1992; Seeger et al. 1993; Drescher et al. 1995; Fradkin et al. 1995; Colavita et al. 1998;

Battye et al. 1999; Kidd et al. 1999; Maloof et al. 1999; Whangbo and Kenyon 1999; Chilton 2006; Okada et al. 2006; Eickholt 2008; Killeen and Sybingco 2008). By means of chemoattraction or chemorepulsion, these guidance molecules lead cells to the correct location. However, temporal regulation of cell migration has been less elucidated.

DTCs provide a paradigm to study the spatiotemporal control of cell migration in *C.elegans*.

C.elegans is a simple model organism with only 959 somatic cells. The life cycle of *C.elegans* is about three days at 20 degree and the brood size of a single hermaphrodite is 200-300. In addition, its transparent body allows researchers to identify individual cells without fixation and staining, which is especially useful for studying cell migration. Although most cell migrations in *C. elegans* occur in embryogenesis, few take place during larval development. Postembryonic migrating cells move along body wall and frequently constitute tissues that are involved in adult-specific function. For example, the descendants of the M mesoblast move circumferentially and longitudinally, contributing additional body wall muscles used for locomotion and egg laying. The descendants of the Z1 and Z4 mesoblasts, which are the DTCs and linker cell in hermaphrodites and males, respectively, migrate longitudinally and circumferentially, determines the adult gonads.

Among all these platform to study cell migration, we choose to study the migration of the distal tip cells (DTCs) for several reasons: first, compared to other cells, the spindle-shaped DTC is of a bigger size, which makes it easier to score under the DIC optics, even without any visible marker. Second, the migration path of the DTC can be reflected by the shape of the gonad arm, as the DTC is located at the tip

of the gonad and guide the extension of the gonad arm during larval development. Thus, mutants with a defective DTC migration path can be easily detected by the abnormal shape of the gonad arm and the specific location of the DTCs can be readily identified under the DIC optics. But the most important one is that, the migration of DTC occurs throughout the larval stage. Furthermore, DTC has specific migration patterns in specific larval stages, which allows us to study the correlation between temporal and spatial regulation of cell migration.

The DTCs are born in the ventral side of the L1 larvae and located at the anterior and posterior ends of the gonad primordium. They undergo a stereotyped migratory path, which are regulated temporally and spatially. Therefore, they provide an ideal model for researchers to study different aspects of cell migration, The DTC migration consists of three sequential linear migratory phases with two right turns between each two phases (Kimble and Hirsh 1979; Hedgecock et al. 1987). In the first phase of migration, the anterior and posterior DTCs start from the ventral midline and migrate along the ventral body wall muscle toward the head and the tail, respectively (Fig.1A). In the second circumferential phase, DTCs migrate from the ventral to dorsal body wall muscle along the inner wall of the epidermis. In the third phase of DTC migration, DTCs turn 90 degree again and migrate along the dorsal body wall muscle until reaching the midbody.

Genes affecting DTC motility and polarity

The activity of *gon-1*, which encodes metalloprotease is required for DTC motility (Blelloch and Kimble 1999). The bHLH transcription factor of Achaete-Scute family, MIG-24, forms heterodimers with HLH-2, an E/Daughterless family bHLH transcription factor, and binds to the *gon-1* promoter to activate the expression of

gon-1 (Tamai and Nishiwaki 2007). In *gon-1* mutants, the DTCs fail to migrate, resulting in a ball-shaped and nonfunctional gonad (Blelloch et al. 1999). Another metalloprotease encoded by *mig-17* is required in the second and the third phases of DTC migration (Nishiwaki et al. 2004). MIG-17 requires to be glycosylated, which involves the activity of MIG-23, a membrane-bound nucleoside diphosphatase (NDPase), to localize to the surface of the gonad where MIG-17 can execute its function properly (Nishiwaki et al. 2004).

The Rac signaling pathway is involved in DTC motility and polarity. The components of this pathway include *ced-2/CrkII*, *ced-5/DOCK180*, *ced-12/Elmo*, which act upstream of *ced-10/Rac* (Wu et al. 2002). Mutants in these genes make DTCs migrate aberrantly in length and polarity.

The guidance control of DTC migration

Migrating cells require guidance signals for proper directions. In most cases, the chemical signals released by the surroundings would lead the way for the migrating cells by means of chemoattraction or chemorepulsion (Hedgecock et al. 1987; Leung-Hagesteijn et al. 1992; Montell 1999; Lehmann 2001). Although little is known about the guidance for the first and the third phases of DTC migration, the mechanism of the ventral-dorsal guidance has been quite well studied.

The circumferential DTC migration requires the UNC-6/netrin (Hedgecock et al. 1990b; Culotti and Merz 1998) system. UNC-6 is a homologue of mammalian netrin in *C.elegans*. The secreted UNC-6/netrin guidance cue is expressed in the ventral side of the worm whereas its predicted receptors UNC-40/DCC and UNC-5 are expressed in the DTCs (Wadsworth et al. 1996; Su et al. 2000b). In *unc-5*, *unc-6* and *unc-40* mutants, the DTCs fail to turn dorsally. They move back to the midbody without the

second dorsal migration. *unc-40* is expressed in the DTC throughout the three migration phases (Chan et al. 1996). In contrast, *unc-5* is transcriptionally upregulated just prior to DTC dorsal turn in the mid-L3 stage (Su et al. 2000a). When DTCs start to transcriptionally upregulate *unc-5*, the ventrally distributed UNC-6 generates a repulsive force via UNC-5/UNC-40 receptor complex and then drives the DTCs to turn dorsally. Besides, a precocious transcriptional activation of *unc-5* by the promoter of *emb-9* cause DTC to make an early dorsal turn, indicating that *unc-5* expression is sufficient for the DTCs to turn dorsally (Su et al. 2000b). All these results together suggest that the timing of *unc-5* expression determines when the DTC turns.

As DTCs move farther and farther from the ventral side during the ventral-to-dorsal migration, they become dependent of the dorsally localized extracellular signal UNC-129/TGF- β , which sensitizes their response against the netrin signal. *unc-129* is expressed in the dorsal, but not ventral, body wall muscle because of the transcriptional repressor *unc-130*, which is present in the ventral, but not dorsal, body wall muscle (Colavita and Culotti 1998; Colavita et al. 1998; Nash et al. 2000). UNC-129 was proposed to help the formation of the heterodimer receptor, UNC-5+UNC-40, which is in charge of the long-range repulsion of UNC-6, by directly binding to UNC-5 for inhibiting UNC-5 from forming homodimers with itself, which is responsible for the short-range repulsion of UNC-6.

The expression timing of the netrin receptor, *unc-5*, is very important for the proper morphogenesis of the *C.elegans* gonad, because *unc-5* expression is sufficient to drive DTC turn dorsally. If the DTC or delays its dorsal migration resulted from the improper expression timing of *unc-5*, the gonad loses its perfect U-shaped and affect the fertility as a result.

After DTCs move from the ventral to dorsal side, they migrate longitudinally back to the dorsal midline. Although this third phase of DTC migration composes one-third of this migration process, the mechanism of its directional control is poorly understood. From the studies of *unc-5*, *unc-6* and *unc-40* mutants, the migration of the third phase, including its timing and the direction, is not affected even when the second phase is not properly executed, *i.e.* DTCs wait till the right time to move back to the midline even without the second ventral-to dorsal migration (Hedgecock et al. 1990b; Su et al. 2000b).

The temporal control of DTC migration

During the migration course, the DTCs make 90 degree turns twice. Both turns are temporally regulated. The first turn, *i.e.* the dorsal turn, which leads DTCs to enter the second phase migration, is executed at the mid-L3 stage; while the second turn, which makes DTCs entering the third from the second migratory phase in the late L3 stage (Fig.1A). Therefore, at the time point of the L3 molt, the gonad would exhibit a reflex caused by these two turns. Compared to the dedicated studies of the heterochronic genes functioning in the temporal programming of the hypodermal seam cells (Ambros 2000; Fielenbach and Antebi 2008), the temporal regulation of DTC migration is little. Thus far, there have been only four heterochronic genes reported to be involved in the temporal regulation of DTC migration, including *lin-42*, *lin-29*, *dre-1*, *daf-12*.

LIN-42 is the *C.elegans* homologue of the Period (Per) family of circadian rhythm protein (Jeon et al. 1999). In *lin-42(RNAi)* mutant, the gonad reflex that is normally observed in the L3 molt is detected in L2 molt, one stage earlier than wild type (Tennessen et al. 2006). In contrast to *lin-42* mutants with precocious reflex,

lin-29(n546);daf-12(rh61rh411), *lin-29(n543);dre-1(dh99)* and *dre-1(dh99);daf-12(rh61rh411)* double mutants have delayed gonadal reflex (Fielenbach et al. 2007). LIN-29 is a transcriptional factor, DAF-12 is a steroid hormone receptor and DRE-1 is an F-Box protein functional related to E3 ubiquitin ligase. Their molecular identities imply that the temporal regulation of the L3 reflex involves different levels of gene regulation such as transcription and protein stability. Moreover, since there is no defect detected in the single mutant of *lin-29*, *dre-1* and *daf-12*, the temporal regulation of DTC migration should be a gene network instead of a linear pathway. But how exactly these genes work in the temporal regulation of DTC migration and how do the link to the spatial regulation is still unknown.



Material and Methods

Strains and Genetics

C. elegans strains were cultured on NGM agar inoculated with *E. coli* OP50 at 20°C (Sulston 1988). The N2 Bristol strain was used as the reference wild-type strain. The mutations used were as follows: LGI, *dpy-24(s71, tk41, tp5* and *tm548)*, *unc-40(e271)*, *lin-29(n546)*; LGIII, *unc-119(ed3)*; LG IV, *unc-5(e53)*, *unc-129(ev557)*; LGV, *dre-1(dh99)*; LGX, *unc-6(rh46)*, *daf-12(rh61rh411)*. The *dpy-24(tm548)* mutant was generated and provided by the Mitani lab. The *dpy-24(tk41)* mutant was isolated from a screen for mutants defective in DTC migration and was kindly provided by K. Nishiwaki (unpublished results). The Hawaiian strain CB4856 was used for single-nucleotide polymorphism (SNP) mapping (Wicks et al. 2001). The strain RW7000 was used for sequence- tagged site (STS) mapping (Williams et al. 1992). Double-mutant strains were constructed by standard methods. The *daf-12* reporter strain AA120 is a kind gift from Dr. Adam Antebi, which was generated by UV-integration of *daf-12GFP* and *lin-15* coinjection marker into *daf-12(rh61rh411)*; *lin-15(n765)* (Antebi et al. 2000).

EMS mutagenesis.

EMS mutagenesis was performed as described previously (Brenner 1974). Worms at about early L4 stage were treated with 47 mM EMS for 4 hrs with gentle agitation at 20°C. The F1 progeny of mutagenized animals were cloned and their F2 progeny were screened for the dorsal clear patched indicative of defects in DTC migration.

72000 haploid genome was screened and found one alleles, *tp5*. After outcrossed twice, *tp5* not only exhibits DTC migration defect but also has a dumpy body shape, suggesting that these two phenotypes are caused by the same mutation.

***dpy-24* cloning and cDNA construction**

s71 was mapped to chromosome I near stP124 by STS mapping. Three factor mapping using *unc-40* and *unc-75* and SNP mapping positioned *s71* within the region between cosmids F45H11 and F37D6. Cosmids covering this region were microinjected into *dpy-24(s71)* mutants. The cosmid F25D7 rescued the dumpy phenotype and DTC migration defects of *dpy-24(s71)* mutants.

To obtain the 5' end of *dpy-24* cDNA, the first three exons were amplified by RT-PCR using the forward primer corresponding to the SL1 sequence and the reverse primer 5' GTTCA TAGGA AGTGT GCATT CTGCT C 3'. The resulting PCR product and the *dpy-24* cDNA fragment from the yk487b7 clone were fused by fusion PCR and subsequently cloned into the vector pGEM-T Easy to generate pYW687, which contains the full-length *dpy-24* cDNA.

Transgenic strains

About 4.6kb fragment upstream of the first ATG of the *unc-5* genomic DNA was amplified by primers 5'-CATTACTGGAATAGAAATTATGATTAGTG-3' (forward) and 5'-GAGAACGGAGCCTCTGAGCCTTG-3'(reverse), then cloned into pGEM-T-easy(invitrogen) and further subcloned into the *gfp* vector pPD95.77 via SphI and Sall site to generate the $P_{unc-5(4.6kb)}::gfp$ construct. $P_{unc-5(4.6kb)}::gfp$ (20ng/ul) was coinjected with the marker $P_{myo-2}::gfp$ (2ng/ul).

An approximately 1kb fragment upstream of the first ATG of the *unc-5* genomic DNA was amplified by primers 5'-GTTTCAGTAGATCTTCAAAG-3' (forward) and 5'-TACTGGAATAGAAATTATGATTAGTG-3' (reverse) and cloned into pGEM-T-easy (invitrogen). The 1 kb fragment was subsequently cloned to the *gfp* vector pPD95.75 via the XmaI site to generate the $P_{unc-5(1kb)}::gfp$ construct. The *gfp* of

the resulting *P_{unc-5(1kb)::gfp}* was replaced by mCherry cDNA to generate the *P_{unc-5(1kb)::mCherry}* construct. *P_{unc-5(1kb)::GFP}* (20ng/ul) or *P_{unc-5(1kb)::mCherry}* (100ng/ul) was coinjected with the marker *P_{myo-2::gfp}* (2ng/ul).

The fragment *P_{dpy-24::dpy-24::gfp}* was generated by fusing two DNA pieces corresponding to the *dpy-24* genomic DNA and the region containing *gfp* and *unc-54* 3'UTR of the pPD95.75 plasmid using the fusion PCR method described by Hobert (Altun-Gultekin et al. 2001). The primers d245'5kb/f (5' GATGG AAAGT TGACC TAAAT GTCGG 3') and d24gfp/r (5' AGTCG ACCTG CAGGC ATGCA AGCTT GGATA ATGCG GCAAT CCGAG GC 3') were used as primers to amplify *dpy-24* genomic DNA. The primers gfp/f (5' AGCTT GCATG CCTGC AGGTC GACT 3') and u543UTR/r (5' AAGGG CCCGT ACGGC CGACT AGTAG G3') were used as primers to amplify the region corresponding to *gfp* and *unc-54* 3'UTR. The two PCR fragments were fused by the fusion PCR method using primers d245'5kbnested/f (5'GCCTG GAAAA CGCCT TTTGA AG 3') and u543UTRnested/b (5' GGAAA CAGTT ATGTT TGGTA TATTG GG 3'). The resulting PCR products *P_{dpy-24::dpy-24::gfp}* (20ng/ul) was coinjected with *unc-119* rescuing plasmid (100ng/ul) into *unc-119(ed3)* to generate the *dpy-24* overexpression worms, *tpEx49*.

Antibodies and Immunostaining

The *dpy-24* cDNA fragment from the plasmid pYW687 was cut with EcoRI and cloned into the pGEX5X-1 vector (GE Healthcare) and pRSET B vector (Invitrogen) at their EcoRI sites to generate the constructs pYW802 and pYW691, respectively. Both GST-DPY-24 and HIS-DPY-24 fusion proteins were present in the inclusion bodies and were purified using standard methods (Harlow and Lane 1988).

Polyclonal antibodies against GST-DPY-24 were generated and affinity-purified

essentially by DPY-24HIS as described (Perrone et al. 1998). Purified antibodies recognized GST-DPY-24 but not GST on a western blot, indicating the specificity of the antibodies against DPY-24. Worm immunostaining was carried out using the protocol as previously described (Finney and Ruvkun 1990), fixed for 1 hr in 4°C, using the purified DPY-24 antibody as the primary antibody (1:100, 4°C overnight) and the RRX-conjugated donkey-anti-rabbit antibody (Jackson ImmuneResearch) as the secondary antibody (1:100, RT for 2 hr). For *lin-29(RNAi);daf-12(rh61rh411)*, 20-30 worms were picked in 6ul distilled water on a gelatin-chromic potassium sulfate subbed slide (Rowse-Eagle et al. 1981) with 1mM Azide and 1mg/ml poly-L-Lysine (from Dr. Satouru Ozawa of Babara Meyer's lab), freeze-cracked, fixed in 95% ethanol and 2% PFA for 10 min respectively. The fixed samples were incubated with DPY-24 antibody (1:1000) for RT overnight, washed by PBSTB (1XPBS, 0.5% Triton X-100, 0.05% Azide, 0.1%BSA) for 3 times and incubated with RRX-conjugated donkey-anti-rabbit antibody (1:1000; Jackson ImmunoResearch) for RT overnight. Samples were mounted with 2ul DABCO anti-bleaching reagent (Fluka) and 1ul DAPI(0.5ug/ml) and observed under Normaski microscopy.

RNA interference

Feeding or injection of RNAi is preformed as previously described (Kamath et al. 2001). RNAi construct of *lin-29* is by amplifying exon 3 to exon 10 of *lin-29* cDNA from yk1430g04 and cloned this fragment into L4440 vector. The RNAi construct of *dpy-24* is from Ahringer RNAi library.

Yeast assay.

Yeast transcriptional reporter assay.

The reporter yeast strain YM4271[*Punc-5::HIS3*] is generated by integrating yeast strain YM4271 with plasmid *Punc-5::HIS3*, which was constructed by subcloning the 1 kb promoter of *unc-5* of *Punc-5::gfp* into pHisi-1. The DAF-12 constructs used in the yeast activation study were generous gifts from Dr. Keith Yamamoto: DAF-12(A1 form), DAF-12 constitutive active form (aa1-500) and DAF-12DBD (aa 100-206) driven by CUP1 promoter in pRS424 (2 μ , TRP). Transformants were selected out by SC-Trp-Ura-His and tested for the transcriptional activation by different concentration of 3AT in the presence of 0.05mM CuSO₄.

Yeast one-hybrid.

The fragments of DPY-24 zinc fingers and DPY-24 Δ zinc finger were PCR-amplified and cloned into pGAD-C1(LEU) to generate GAL4-activation domain fusion, whereas DPY-24 full length was directly subcloned from pGEM-T-easy. For there were no proper cloning site for subcloning DAF-12 fragments from pRS424 to pGAD-C1, we used DAF-12 fragments in pRS424 as the templates to amplify DAF-12, DAF-12 constitutively active form and DAF-12DBD and cloned it into pGAD-C2. All of these GAL4-activation domain fusion constructs were transformed into the yeast reporter strain YM4271 [*Punc-5::HIS3*], selected out by SC-Leu-His plates and tested for the strength of protein-DNA interaction by different concentration of 3AT.

Results

***dpy-24* mutants are defective in DTC migration**

To understand the mechanism of cell migration, a genetic screen for the mutants defective in DTC migration was conducted. From this screen, *tp5* mutant was isolated. A subsequent non-complementation test and mapping data showed that *tp5* was allelic to the previously identified mutation *dpy-24(s71)*, revealing that *dpy-24* plays a role in DTC migration. Further genetic analysis showed that two other alleles *tk41* and *tm548*, isolated by Kiyoji Nishiwaki and Shohei Mitami's labs, respectively, were allelic to *dpy-24(s71)*. All four alleles share a similar set of defects, which include DTC-migration defects (Figure 1), a weak dumpy phenotype (Figures 2A and 2B), and a partially penetrate embryonic lethality (C.Y. Chao and Y.C. Wu unpublished results).

To characterize the function of *dpy-24* in DTC migration, we analyzed the DTC migration defect of all *dpy-24* mutant alleles that were available, including *s71*, *tp5*, *tk41* and *tm548*. Most *dpy-24* DTCs exhibited a common feature: the ventral-to-dorsal phase II migration was initiated at the position closer to the midbody than that of wild type (Figures 1C-E). Some of these DTCs were found to migrate obliquely with respect to the dorsoventral axis until they reached the dorsal muscle (Figure 1C). Such a migratory route may be attributed to simultaneous execution of centrifugal phase I and dorsal phase II migrations, suggesting a precocious initiation of dorsalward phase II turning. In addition to the abnormal initiation of phase II migration, some *Dpy-24* DTCs reverse the direction of centripetal phase III migration (Figure 1E). These DTCs fail to move back towards the mid-body and rather migrate towards the end of the body, suggesting a role of *dpy-24* in the control of phase III migration direction.

To facilitate characterization of the *Dpy-24* DTC migration phenotypes, we

tentatively define the defect showing only the abnormal initiation of phase II migration as class 1 (Figures 1C and D) and the defect with an additional abnormality of the reversed phase III migration direction as class 2 (Figure 1E). The defect of DTCs, which move towards the end of the body without making any turn, is defined as class 3 (Figure 1F). The percentage of DTCs in each class in all four *dpy-24* mutant alleles was listed in Table 1.

***dpy-24* mutants have a precocious DTC dorsal turn at the early L3 stage**

As *dpy-24* mutants had a short phase I migratory path, we examined if this may be attributed to slow migration of DTCs. We scored DTC positions relative to the hypodermal Pn.P and seam cell nuclei in wild-type and *dpy-24* worms. At L2 molt, the anterior DTCs were located between P4.p and P5.p and posterior DTCs between P7.p and P8.p in wild type. About six hours later, anterior DTCs moved to the region between V1.pppp and V2.papp, and posterior DTCs between V4.pppp and V6.papp (Figure 3). A similar result was observed in *dpy-24* mutants, indicating that DTC migration was not significantly slowed (Figure 3).

To understand the cause leading to the abnormal position of ventral-to-dorsal phase II turning in *dpy-24(s71)* mutants we performed the time-course analysis of DTC migration in wild-type and *dpy-24* worms. The division stages of the vulval precursor cell P6.p were used as temporal developmental markers. The P6.p is born in mid-L1. It undergoes three rounds of cell division during the L3 stage and gives rise to eight descendents that constitute the vulva (Sulston and Horvitz 1977). The timing of each P6.p division is similar in wild-type and *dpy-24* animals. We found that more than 90% DTCs underwent ventral-to-dorsal phase II migration at the four-P6.p cell stage in wild type and that no DTC made a dorsal turn prior to P6.p cell division

(Figure 4). However, in *dpy-24* mutants 36% anterior DTCs and 66% posterior DTCs had turned dorsalward before P6.p divided (Figure 4). These results show that *dpy-24* mutations cause the DTCs to undergo a precocious dorsal turn, leading to uncoupling of developmental timing in gonadogenesis with the rest of reproductive system such as valva at the L3 stage.

In addition to developmental age, we also measured and compared the chronological age of the wild-type and *dpy-24* worms when their DTCs underwent a ventral-to-dorsal phase II turning. On average, the *dpy-24* and wild-type DTCs turned dorsalward 32.5 and 36 hours after hatch, respectively (Figure 5). The temporal difference between *dpy-24* and wild-type DTC dorsalward turnings was about one third of the L3 developmental period. Taken together, these data show that the DTCs of *dpy-24* mutants undergo a precocious dorsal turn. Therefore, *dpy-24* plays an important role in the timing control of gonadogenesis.

DPY-24 encodes a protein with a PR domain and five zinc fingers related to the mammalian protein Blimp-1 and PRDI/BF1

We mapped *dpy-24* to chromosome I between *lin-11* and *unc-75* by RFLP and SNP mapping. We cloned *dpy-24* by germline transformation using cosmids spanning in this interval. We found that the cosmid clone, F25D7, rescued the DTC migration defect and the dumpy phenotype of *dpy-24(s71)* mutants (Figure 6). The genomic DNA fragments corresponding to 5 predicted open reading frames of F25D7 were individually amplified by long PCR and tested for their abilities to rescue *dpy-24(s71)* mutants. Only F25D7.3 rescued the DTC-migration defect and the dumpy phenotype (Figure 6). In addition, RNA interference (RNAi) of F25D7.3 phenocopied *dpy-24(s71)* mutants. These results indicate that F25D7.3 corresponds to the *dpy-24*

gene.

DPY-24 is similar to mouse B lymphocyte-induced maturation protein 1 (Blimp-1) and human positive regulatory domain I-binding factor (PRDI-BF1) with 27 % and 26 % identities, respectively, throughout their entire lengths (Figure 7). Both Blimp-1 and PRDI-BF1 have been shown to act as transcriptional repressors essential for the terminal differentiation of B cells into immunoglobulin-secreting plasma cells (Turner et al. 1994). DPY-24, like Blimp-1 and PRDI-BF1, was predicted to contain a PR (Positive Regulatory) domain, a nuclear localization signal (NLS) and five Kruppel-type [(Cys)₂-(His)₂] zinc fingers (Figure 7). The zinc fingers of both Blimp-1 and PRDI-BF1 have been shown to bind to target DNA directly and are essential for their transcriptional repression activities (Lin et al. 1997; Piskurich et al. 2000; Ghosh et al. 2001). The PR domain shares high similarity with the SET domain, which is found in methyltransferase protein. However, the PR domain of Blimp-1 and PRDI-BF1 do not contain the NHSC(I) sequence required for the catalytic activity of methyltransferase and therefore is thought to lack the methyltransferase activity. (Huang et al. 1998; Kouzarides 2002).

We identified molecular lesions of *dpy-24* alleles, confirming that we have correctly identified the *dpy-24* gene. Alleles *s71*, *tk41* and *tp5* have non-sense mutations in codons 281, 381 and 434, respectively, and are predicted to encode truncated proteins without zinc fingers (Figure 7). Allele *tm548* is an 810 bp deletion, removing parts of exon 3 and intron 3 (Figure 7). The deletion may result in a truncated and hybrid DPY-24 protein, which contains the first 254 amino acids of DPY-24 and additional 17 amino acids encoded by the third intron.

DPY-24 is transiently present in DTCs before dorsal turn but absent after dorsal turn.

We raised polyclonal antibodies against recombinant DPY-24 protein (see Materials and Methods). Affinity-purified DPY-24 antibodies were used to stain whole-mount animals. DPY-24 was detected in anterior, lateral and posterior hypodermal cells in embryos and larvae (Figures 8A-8D). The expression of *dpy-24* in hypodermal cells is consistent with the dumpiness of *dpy-24* mutant, suggesting the role of *dpy-24* in the regulation of the body size.

DPY-24 was also observed in vulval and intestinal cells (Figures 8C and 8E). Importantly, DPY-24 was detected in the DTCs (Figure 8F), consistent with its cell autonomous function in the control of DTC migration. In all stained cells DPY-24 was localized to the nuclei. None of the staining signals described above was detected in *dpy-24(s71)* mutants, indicating the specificity of antibodies to DPY-24 in these cells.

Interestingly, *dpy-24* expression in the DTCs was detected only during centrifugal phase I migration, but not during or after dorsal phase II migration (Figure 9). This finding together with the Dpy-24 phenotype of precocious dorsal phase II migration indicates that DPY-24 functions in DTCs during phase I migration to prevent their precocious dorsal phase II turning and that the timely disappearance of DPY-24 may allow the DTCs to initiate their dorsal phase II migration.

Constitutive expression of *dpy-24* delays dorsal phase II migration

We further investigated the significance of *dpy-24* downregulation and its effect on the initiation of DTC dorsal phase II migration. To this end, we over-expressed *dpy-24* using the translational fusion construct $P_{dpy-24}dpy-24::gfp$, in which *gfp* is fused to the 3' end of *dpy-24* cDNA and is controlled by the endogenous *dpy-24*

promotor P_{dpy-24} . In the resulting transgenic line *tpEx49* the DPY-24::GFP was not properly down-regulated and persisted throughout larval development (Figure 10I). The constitutive expression of *dpy-24::gfp* in the late larval stage, when *dpy-24* was normally absent, delayed in the dorsal phase II migration of 76.8% and 49.2% of anterior and posterior DTCs, respectively. The affected DTCs failed to turn dorsalward and, instead, remained in the centrifugal phase I migration, even at the L4 and adult stages (Figures 10H). This phenotype was in contrast to the precocious migration phenotype resulted from *dpy-24* loss-of function mutations (Table 1 and Figure 1). Collectively, these data show that the DPY-24 level determines the temporal fate of DTCs. Low level of DPY-24 accelerates the initiation of DTC dorsal migration, whereas high level of DPY-24 brakes dorsalward turning. In young larvae, the DTCs have high level of DPY-24 and undergo centrifugal phase I migration. The timely disappearance of DPY-24 in the L3 stage allows the spatial fate of the DTCs to switch from centrifugal phase I to dorsal phase II. *dpy-24* thus plays a pivotal role in coordinating the temporal and spatial control for proper DTC migration.

The precocious dorsal turn of *dpy-24* mutants requires canonical Netrin/Unc-5 pathway.

Dorsal migration of DTCs depends on UNC-6 netrin and its receptors UNC-5 and UNC-40 (Hedgecock et al. 1990b; Leung-Hagesteijn et al. 1992; Chan et al. 1996; Wadsworth et al. 1996). Mutations in *unc-5*, *unc-6* or *unc-40* partially block the ventral-to-dorsal phase II turning of the DTCs, resulting in the “no dorsal turn” phenotype. For example, 48% anterior DTCs and 83 % posterior DTCs fail to turn dorsalward in *unc-5* mutants (Table 2). UNC-129, a recently identified UNC-5 ligand, also regulates ventral-to-dorsal DTC migration (Colavita et al. 1998; MacNeil et al.

2009). Although the *unc-129* null allele does not cause any DTC migration defect, it aggravates the dorsal phase II migration defect of the *unc-5* (*e152*) hypomorph (MacNeil et al. 2009). To investigate if the precocious DTC dorsal turn of *dpy-24* mutants may depend on *unc-5*, *unc-6*, *unc-40* or *unc-129* we analyzed the DTC migration patterns of *dpy-24; unc-5*, *dpy-24; unc-6* and *dpy-24 unc-40* and *dpy-24; unc-129* double mutants. Approximately 77% anterior DTCs and 93 % posterior DTCs underwent a precocious dorsal turn in *dpy-24(s71)* mutants (Table 2). In *dpy-24(s71); unc-5* double mutants, almost all anterior and posterior DTCs (98% each) failed to turn dorsalward and no precocious dorsal turn was observed (Table 2). Similar results were obtained in *dpy-24; unc-6*, *dpy-24; unc-40* and *dpy-24; unc-129* double mutants. These findings together indicate that the precocious dorsal migration of Dpy-24 DTCs required the *unc-5*-mediated pathway.

Surprisingly, mutations in any of *unc-5*, *unc-6*, *unc-40* and *unc-129* significantly enhanced the phenotype of the reversed direction of centripetal phase III migration in the *dpy-24* mutant background. For example, the defect with reversal of centripetal phase III migration direction in *dpy-24(s71)* mutants (classes 2 and 3 in Table 1) was augmented by the *unc-5(e53)* mutation from 58% to 98% in anterior DTCs and from 13% to 31 % in posterior DTCs (Table 2). Similar results, but to a lesser extent, were observed in *unc-6*, *unc-40* and *unc-129* mutations. These data together indicate that *dpy-24* acts with the *unc-5* pathway, likely in parallel, to control the direction of centripetal phase III migration.

***dpy-24* represses *unc-5* transcription to prevent precocious dorsal turn of DTCs.**

We then look for the mechanism by which *dpy-24* negatively regulates the dorsalward turning of the DTCs. Previous studies show that precocious activated

unc-5 by *emb-9* promoter is sufficient to drive DTC turn dorsally (Hedgecock et al. 1990a; Su et al. 2000a). However, *emb-9* is not only expressed in DTC, but in body wall muscles and hypodermal cells. To further investigate whether this phenomenon is cell autonomous or not, we use $P_{lag-2}::unc-5$ to drive *unc-5* precociously and specifically in DTC. We found that $P_{lag-2}::unc-5$ as well could generate precocious dorsal turns as *dpy-24* mutation (Table 1). In addition, the phenotype of precocious DTC dorsal turn in *dpy-24* mutants requires *unc-5* (Table 2). These observations in combination with the previous findings that Blimp-1 and PRDI-BF1 function as transcription repressors prompted us to hypothesize that *dpy-24* may prevent DTCs from precocious dorsal turn by transcriptional repression of *unc-5*.

The *unc-5* promoter $P_{unc-5(4.6)}$, which is the 4.6 kb genomic fragment upstream of exon 2, contains sufficient regulatory sequence to rescue the DTC migration and axon guidance defect of *unc-5* mutants when fused to an *unc-5* cDNA (Hamelin et al., 1993; Su, 2000). We narrowed the promoter fragment down to 1kb. The resulting $P_{unc-5(1kb)}$ promoter, like $P_{unc-5(4.6kb)}$, is expressed in the DTCs during and after, but not before, their dorsal turn. The *unc-5* transcription pattern is complementary to the DPY-24 protein pattern, in which DPY-24 is only present prior to DTC dorsal turn, supporting the notion that DPY-24 represses *unc-5* transcription (Figure 9). To investigate if there is causal relationship between the levels of DPY-24 protein and *unc-5* transcription, we further examined the effect of the *dpy-24* mutation and overexpression on *unc-5* transcription in worms carrying the transgene $P_{unc-5(1kb)}gfp$.

In wild-type DTCs, neither *gfp* expression nor DTC dorsal turn was observed in the early L3 stage (Figures 10A and 10B). In contrast, *dpy-24* mutants at the same developmental stage exhibited premature DTC dorsal turn and concomitant precocious *gfp* expression (Figures 10C and 10D). Therefore, *dpy-24* negatively

regulates *unc-5* transcription in the DTCs and that premature *unc-5* up-regulation may be responsible for the precocious DTC dorsal migration in *dpy-24* mutants.

We further assess the effect of constitutive *dpy-24* expression on *unc-5* transcription at the time when DPY-24 is normally absent in the transgenic worm *tpEx49*. The reporter construct $P_{unc-5(1kb)}::mcherry$, in which the expression of the red fluorescent protein mcherry was controlled by $P_{unc-5(1kb)}$, was used to monitor the *unc-5* transcriptional level. In the DTCs with a persistent DPY-24::GFP signal at the L4 stage, neither $P_{unc-5(1kb)}::mcherry$ expression nor DTC dorsalward turning was observed (Figures 10H-J). In contrast, in the control DTC at the same stage, which showed a normal downregulation of DPY-24::GFP, both *unc-5* transcription, as monitored by the $P_{unc-5(1kb)}::mcherry$ transgene, and DTC dorsalward phase II turning were observed (Figures 10 E-G). Thus, ectopic expression of *dpy-24* is sufficient to repress *unc-5* transcription and blocks DTC dorsal turn. The phenotype caused by constitutive *dpy-24* overexpression is opposite to that of *dpy-24* mutants. These data together confirm the causal relationship of the reciprocal expression levels of *dpy-24* and *unc-5* in the DTCs and support the notion that *dpy-24* negatively regulates *unc-5* transcription to prevent the DTCs from precocious dorsal turn.

The zinc fingers of DPY-24 bind directly to the *unc-5* promoter at D1 and D2 sties.

The yeast one-hybrid system was utilized to verify the direct interaction between DPY-24 and the *unc-5* promoter. The $P_{unc-5(1kb)}::HIS$ reporter was integrated into the yeast strain YM4271, and different DPY-24 cDNA construct encoding full length DPY-24 (DPY-24FL), the zinc finger domain (DPY-24ZF) and truncated DPY-24 without the zinc finger domain (DPY-24 Δ ZF) were transformed into the yeast

reporter strain YM4271 [$P_{unc-5(1kb)}::HIS$] individually. The direct interactions were only detected in the yeast reporter transformed with DPY-24FL and DPY-24ZF, but not in that with DPY-24 Δ ZF (Fig.11A-C) Therefore, DPY-24 could bind to *unc-5* promoter directly through its zinc fingers.

To find the exact binding site of DPY-24 on *unc-5* promoter, we collaborated with Dr. Yi-Sheng Cheng. Using the homology modeling, he found that in the DPY-24-DNA complex model, the amino acids Gln519, Asn522, Gln 547, His550, Asn578, Gln603 and His606 located in the zinc finger motifs are predicted to interact with DNA. A further examination of the DPY-24ZF-DNA complex model suggests a conserved core sequence GAAAA, which is similar with the reports of Blimp-1 and PRDI-BF1 binding sequence GAAAG.

Inspection of the 1kb fragment of the *unc-5* promoter revealed two potential DPY-24 binding sites located between -500 and -440 bp, GAAAATGAAAG and GAAAGAGAAAG. We named them D1 and D2, respectively (Figure 11D). Later in our lab, the direct binding of DPY-24ZF to the D1 and D2 sites on *unc-5* promoter were confirmed by electrophoretic mobility shift assay (EMSA) (Chun-Yi Cho and Yi-Chun Wu, unpublished data).

It is difficult to reveal the biological significance of D1 and D2.

To investigate the biological function of D1 and D2, the *unc-5* promoter mutated on D1 and D2 sites, $P_{unc-5(1kb)m12}::gfp$, and the wildtype *unc-5* promoter, $P_{unc-5(1kb)WT}::gfp$, were constructed and injected into N2 respectively. We checked DTCs of early L3 stage, and expected to detect the early expression of $P_{unc-5(1kb)m12}::gfp$ resulted from the de-repression of DPY-24. To our surprise, there was no difference between $P_{unc-5(1kb)m12}::gfp$ and $P_{unc-5(1kb)WT}::gfp$ in DTCs throughout

all stages.

It has been reported that Blimp-1 (CIITA suppressor) shared the same binding site with IRF (CIITA activator) on the promoter of CIITA. When researchers mutated the Blimp-1 binding site, they also destroyed the binding site of the activator IRF. Therefore, no difference was detected between the mutated promoter and the control promoter, because there was neither activation nor suppression. It is quite like the situation we met in phase I, however, it can't explain why $P_{unc-5(1kb)m12::gfp}$ could still be activated when entering phase II.

It is also possible that maybe there is other suppressors besides *dpy-24*. Therefore, although $P_{unc-5(1kb)m12::gfp}$ is released from the suppression of DPY-24, there might be other suppressors to suppress it to express in early L3. However, the fact that the percentage of DTCs with the precocious dorsal turn is high in *dpy-24* single mutant suggests that *dpy-24* alone is sufficient to suppress *unc-5* in early L3.

The lack of *unc-5* activators might be the reason of the incapability of $P_{unc-5(1kb)m12::gfp}$ to turn on in DTCs in early L3. However, in *dpy-24* mutants, DTCs could make their dorsal turn in early L3 indicating that the activators are readily exist in early L3. Therefore we speculate that *dpy-24* might suppress *unc-5* activators as well as *unc-5* in phase I. Therefore, in *dpy-24* mutants, when there is no DPY-24 in early L3, the *unc-5* activators are able to activate *unc-5* and precociously drive DTCs turn dorsally. But in N2 with $P_{unc-5(1kb)m12::gfp}$, although $P_{unc-5(1kb)m12::gfp}$ is no longer suppressed by DPY-24, the endogenous DPY-24 could still suppress the *unc-5* activators. Until DPY-24 is disappeared in mid L3, the *unc-5* activators could be released and activate *unc-5* thereafter. Nevertheless, we can't test this hypothesis in *dpy-24* mutant since there will be no DPY-24 suppressor, so the difference between $P_{unc-5(1kb)m12::gfp}$ and $P_{unc-5(1kb)WT::gfp}$ is still unable to tested.

Down-regulation of DPY-24 is controlled by the heterochronic genes *dre-1*, *daf-12* and *lin-29*

To identify genes responsible for downregulation of DPY-24 in DTCs, we sought for mutants with a phenotype resembling that of constitutive expression of *dpy-24*. The heterochronic genes, *daf-12*, *dre-1* and *lin-29*, function redundantly specify the L3 fate of DTCs, including their dorsal migration (Fielenbach et al. 2007). The double and triple mutations, but not single mutations, of the three genes delay or even block the initiation of dorsal phase II migration. We confirmed this result (Table 3) and further examined if these genes may be responsible for DPY-24 down-regulation by immunostaining the double mutants with the anti-DPY-24 antibodies. In the wild-type control, DPY-24 was never observed in the DTCs at the L4 stage (n=62) (Figure 12). In contrast, persistent DPY-24 protein was observed in the DTCs of all *lin-29(n546)*; *dre-1(dh99)* double mutants at the L4 stage (n=30) (Figure 12). However, in *dre-1(dh99)*; *daf-12(rh61rh411)* mutants only 3% of DTCs showed persistent DPY-24 protein at the L4 stage and the signal was much less intense than that of *lin-29(n546)*; *dre-1(dh99)* mutants at the same stage (n=106) (Figure 12). So is the situation in *lin-29(n546)*; *daf-12(rh61rh411)*. These results indicate that *lin-29*, *dre-1* and, to a lesser extent, *daf-12* work together to down-regulate DPY-24 in the L3 stage.

Furthermore, we generated triple and quadruple mutants to examine the genetic interaction between *dpy-24* and the heterochronic genes *daf-12*, *dre-1* and *lin-29*. A very low percentage of *dpy-24* anterior DTCs exhibited a “no turn” phenotype (class 3 in Figure 1F and Table 1), which superficially resembles the DTC migration defect caused by delay of DTCs reflex in *lin-29*; *dre-1*, *lin-29*; *daf-12* and *dre-1*; *daf-12* double mutants (*dre-1* paper and our observations). However, these Dpy-24 DTCs showed an abnormally high level of *unc-5* transcription as revealed by the

transcriptional *P_{unc-5}:gfp* fusion transgene, arguing against the possibility that their “no turn” phenotype is caused by delay in DTC reflex as those of *lin-29; dre-1*, *lin-29; daf-12* and *dre-1; daf-12* double mutants. For simplicity, we only analyzed the posterior DTCs of triple and quadruple mutants of *dpy-24*, *daf-12*, *dre-1* and *lin-29*. We found that the *dpy-24* mutation partially suppressed the retarded dorsal migration phenotype of posterior DTCs in double and triple mutants of *lin-29*, *dre-1* and *daf-12* (Table 3). Reciprocally, the precocious phenotype of *dpy-24* mutants is also partially suppressed by the double and triple mutations of *lin-29*, *dre-1* and *daf-12*. Thus, in the centrifugal phase I migration *dpy-24* may act upstream of or parallel to *lin-29*, *dre-1* and *daf-12*. When the DTCs switch from the centrifugal phase I migration to dorsal phase II migration, *dpy-24* may function downstream of or parallel to *lin-29*, *dre-1* and *daf-12*. Intriguingly, *dre-1; daf-12* double mutants show a very low penetrance of persistent DPY-24 staining at the L4 stage, when DPY-24 is supposed to be absent in wild type, but their phenotype of retarded DTC migration is strongly suppressed by the *dpy-24* mutation. It is possible that DPY-24 is present in *dre-1; daf-12* mutants at the L4 stage to cause the retarded phenotype but its level is under our antibody detection limit. Alternatively, but not exclusively, *dpy-24* may be regulated by *daf-12; dre-1* together at the activity level.

DAF-12 activates *unc-5* transcription

As mentioned previously, *unc-5* transcription is up-regulated during DTC dorsal turn in L3. We sought for the transcription activator(s) responsible for *unc-5* up-regulation. The fact that *daf-12; lin-29* double mutants show retarded DTC reflex prompt us to examine if *daf-12* and *lin-29* may regulate *unc-5* transcription.

DAF-12 is a nuclear hormone receptor. Without receiving the hormonal signal,

DAF-12 binds to co-repressor DIN-1 and inhibits transcription (Ludewig et al. 2004). After binding with the hormone, DAF-12 changes its role to a transcription activator. Previous studies show that *unc-5* transcription is inhibited by the *daf-12(rh84)* mutation, which results in an amino acid substitution in the ligand-binding domain. Thus, this mutant form (*rh84*) of DAF-12 protein may not be responsive to the positive ligand signal and therefore behaves in a dominant negative fashion. We tested whether DAF-12 could bind to the *unc-5* promoter by using the yeast one-hybrid assay. To this end, cDNA fragments corresponding to full-length DAF-12 (DAF-12FL), truncated DAF-12 without the ligand-binding domain [DAF-12(gf)] and DAF-12 DNA binding domain (DAF-12DB) are fused to the GAL-4 activation domain (AD) and the fusion construct were introduced to the yeast strain carrying the reporter HIS gene under the control of the *unc-5* promoter. All forms of DAF-12 showed strong interaction with the *unc-5* promoter, including DAF-12 full length, DAF-12 constitutive form and DAF-12 DNA binding domain (Figure 13). The reason that full-length DAF-12 (DAF-12FL) can bind to the *unc-5* promoter may be attributed to lack of *din-1*-like repressor in yeast.

To further investigate whether DAF-12 itself could activate *unc-5* promoter, we introduced full-length and truncated *daf-12* cDNA constructs without the activation domain (AD) into the yeast strain with the same $P_{unc-5}::HIS$ reporter gene. It was found that DAF-12 constitutive active form itself could activate *unc-5* promoter, while there was no direct activation by DAF-12 full length or DAF-12 DNA binding domain (Figure 14).

LIN-29 activates *unc-5* transcription

We further examine if LIN-29 could functions as *unc-5* transcription activator. To

this end, we introduced the transcriptional reporter $P_{unc-5(1kb)}::gfp$ to $daf-12(rh61rh41)$ and $lin-29(RNAi); daf-12(rh61rh41)$ mutants. In $daf-12(rh61rh41)$ mutants, the expression of $P_{unc-5(1kb)}::gfp$ was observed in 33.7% of DTCs after the L3 molt; however, in $lin-29(RNAi); daf-12(rh61rh41)$ double mutants, no $P_{unc-5(1kb)}::gfp$ expression was detected in the DTCs after the L3 molt (Figure 15). Therefore, $lin-29$ is involved in the transcriptional up-regulation of $unc-5$, either directly or indirectly. Consistently, the initiation of $lin-29$ transcription is reported to coincides with the initiation of DTC dorsal turn (Bettinger et al. 1996).

To further examine if there is causal relationship of LIN-29 presence and $unc-5$ transcription at the time of DTC dorsalward turning, we precociously expressed $lin-29$ using the transgene $P_{lag-2}::lin-29$ in which $lin-29$ transcription is controlled by the $lag-2$ promoter, P_{lag-2} , during DTC phase I migration. The $P_{unc-5(1kb)}::gfp$ reporter was introduced to the strain to monitor the transcription level of $unc-5$. As we expected, in the two resulting transgenic lines, 27% and 9.5% of the DTCs made their dorsal turn precociously. Furthermore, 14% and 8% of DTCs in early L3 stage were detected with the precociously-activated $P_{unc-5(1kb)}::gfp$, respectively (Table 4). Therefore, the early-expressed LIN-29 could turn on $unc-5$ expression precociously and drive DTC to make a precocious dorsal turn.

Several LIN-29 binding sites were found in the 1kb region of $unc-5$ promoter, and these sites have been verified by the EMSA experiment using the zinc fingers of LIN-29 (Chun-Yi Cho and Yi-Chun Wu, unpublished data). However, whether LIN-29 could directly activate $unc-5$ *in vivo* requires further investigation.

DPY-24 transcriptionally represses $lin-29$ in phase I DTC migration

The fact that $lin-29$ is sufficient to activate $unc-5$ raised a question that how

dpy-24 suppresses *lin-29* to activate *unc-5* in the phase I of DTC migration since *lin-29* is already expressed in DTC during the early L3 stage. The binding sites of DPY-24 and LIN-29 on the 1kb region of the *unc-5* promoter are neither close nor overlapping, so it is not likely that *dpy-24* suppress *lin-29* by hindering LIN-29 binding on the *unc-5* promoter. We then ask if *dpy-24* could suppress the expression of *lin-29*.

As mentioned previously, the expression of *lin-29* started from early L3. However, when the transgenic animals carrying *P_{lin-29}::gfp* were fed with the bacteria producing *dpy-24* double-stranded RNA, the expression of *P_{lin-29}::gfp* in DTCs was detected one-stage earlier, from early L3 stage to early L2 stage (Figure 16). Furthermore, the intensity of *P_{lin-29}::gfp* in DTCs was enhanced largely in the *dpy-24* knocked-down animals. Therefore, *dpy-24* not only represses *unc-5* transcription, likely by direct binding to its promoter, but also inhibits the expression of the *unc-5* activator LIN-29 to keep *unc-5* transcription low enough to prevent DTC from precocious dorsal turn.

These results in combination with our immunostaining result that *lin-29* acts with *dre-1* or *daf-12* to down-regulate the DPY-24 level, show that there exists a mutual suppression between *dpy-24* and *lin-29*. Prior to the L3 stage, the DPY-24 level is high and therefore inhibits *lin-29* and *unc-5* transcription, keeping the DTCs from turning dorsalward. In the mid L3 stage, *lin-29* cooperates with *daf-12* and *dre-1* to down-regulate the level of DPY-24 and hence relieves the transcriptional repression of *unc-5*, which leads to DTC dorsal turn.

Discussion

A functional link between a transcription factor and a guidance receptor

Although there are extensive studies about how the transcription factors or the guidance receptors control the directionality of cell migration or axonal outgrowth, few reports are establishing the functional link between the regulation of the transcription factors and the expression of the guidance receptors. Even-skipped in *Drosophila* has given a good example. Based on the positive correlation between *eve* and *Unc-5* in expression pattern and mutant phenotype, the authors proofed the functional link between *eve* and *Unc-5* that *eve* regulates *Unc-5* expression in dorsal-MSN motor neurons for their dorsal projection (Labrador et al. 2005). In addition to *eve* and *Unc-5*, the expression of *Drosophila* Robo receptors in interneurons is regulated by Lola transcription factor, and so does Lim1 regulate the expression of EphA4 receptors to control the guidance of LMC motor neurons in mice (Crownier et al. 2002). Nevertheless, all of these examples were proofed genetically, and whether these transcription factors directly regulate the expression of the guidance receptors requires further investment. Therefore, in this report, we provided the first example of the direct regulation between a transcription factor and a guidance receptor in a particular cell. We characterized a new gene, *dpy-24*, which controls the timing of DTC dorsal migration by transcriptionally suppressing the precocious activation of *unc-5*.

dpy-24 is a heterochronic gene

Mutations in *dpy-24* cause precocious ventral-to-dorsal phase II turning of the DTCs in the early L3 stage. In contrast, constitutive expression of *dpy-24* in the DTCs in late L3 and L4, at which DPY-24 is normally absent, delays the initiation of dorsal

phase II migration. These results indicate that the *dpy-24* level controls the temporal identity of DTCs and that *dpy-24* negatively regulates the timing of DTC dorsal phase II migration. The heterochronic gene *lin-42* controls the timing of gonadogenesis and epidermal development (Jeon et al. 1999; Tennessen et al. 2006). Inactivation of *lin-42* by RNAi leads to precocious dorsal phase II migration one larval stage early at the L2 stage (Tennessen et al., 2006). Although in *dpy-24(s71)* mutants DTCs underwent a precocious dorsal turn in early L3, no premature dorsal turn was observed during L2 (n=150) or at L2 molt (n=34). Nevertheless, *lin-29* expression, which is normally initiated at the L3 stage (Bettinger et al. 1996), is precociously activated at the L2 stage in the *dpy-24(s71)* mutant, indicating that the *dpy-24* mutation causes a partial transformation of the DTC fate from L2 to L3 and that *dpy-24* is a heterochronic gene. Consistent with a role of *dpy-24* in temporal DTC fate transformation, the mutation in *dpy-24* is able to suppress the heterochronic phenotype of DTC migration in double or triple mutants of *lin-29*, *dre-1* and *daf-12* (Table 3). However, despite that *lin-29* transcription is precociously turned on by the *dpy-24* mutation at the L2 stage, it is insufficient to lead to premature DTC dorsal turn in L2. This may be attributed to the absence of other positive regulators that are required to work together with *lin-29* to promote the premature dorsal turn at the L2 stage and/or the presence of negative regulators that counteract the effect of *lin-29* to repress dorsal turn at the L2 stage in *dpy-24* mutants. Therefore, the *lin-42* mutation appears to result in complete temporal transformation of DTCs from L2 to L3, perhaps by activating multiple components required for the L3-specific gonadogenesis. In contrast, *dpy-24* mutations lead to precocious initiation of a subset of components, such as *lin-29* transcriptional upregulation, required for temporal fate transformation from L2 to L3.

Transcriptional control of *unc-5*

The disappearance of DPY-24 from the DTCs coincides with *unc-5* transcriptional up-regulation and initiation of DTC dorsal turn. Mutations in *dpy-24* lead to precocious *unc-5* transcription and DTC dorsal turn, whereas forced constitutive expression of *dpy-24* causes delayed *unc-5* transcription and DTC dorsal migration. These results together demonstrate that *dpy-24* negatively regulates *unc-5* transcription to prevent DTCs from precocious dorsal turn.

Upon disappearance of DPY-24, LIN-29 and DAF-12 are potential activators responsible for the transcription activation of *unc-5*. In *daf-12;lin-29* double mutants almost all DTCs fail to express *unc-5* and to migrate dorsalward (Table3, Huang, T.F. and Wu, Y.C., unpublished results), suggesting DAF-12 and LIN-29 may positively regulate *unc-5* transcription during the temporal regulation of dorsal phase II migration. In addition, the consensus sequence of DAF-12 binding site has been previously identified (Shostak et al. 2004) and found to be present in the *unc-5* promoter (C.Y. Chao and Y.C. Wu, unpublished results). Although the binding site of LIN-29 has not yet been revealed, we used homology modeling to predict the zinc fingers of LIN-29 on the basis of its similarity to the yeast zinc finger protein ZAZF1 whose DNA binding sequence has been identified. Both predicted DAF-12 and LIN-29 binding sequences are present in the *unc-5* promoters of *C. elegans* and related species (Chao, C.Y. and Wu, Y.C., unpublished results), suggesting direct involvement of DAF-12 and LIN-29 in *unc-5* transcriptional activation.

In *dpy-24* mutants, a small fraction ($\leq 10\%$) of anterior, but not posterior, DTCs fail to migrate dorsalward, suggesting a minor role of *dpy-24* in promotion and/or execution of dorsal phase II migration. Further supporting this notion, the *dpy-24(s71)* mutation significantly increases the percentage of the no-dorsal-turn phenotype from

42% to 98% in anterior DTCs of *unc-5(null)* mutants (Table 2). A similar enhancement effect by the *dpy-24* mutation was observed in posterior DTCs, albeit to a lesser extent, and in DTCs of mutants defective in the other component of the netrin pathway (Table 2). These results suggest a positive role of *dpy-24* in parallel to the netrin pathway in the promotion and/or execution of dorsal phase II migration of DTCs and indicate that *dpy-24* has targets other than *unc-5* in regulation of dorsal phase II migration.

***dpy-24* likely acts in parallel to *unc-5* to control the direction of the centripetal phase III migration of DTCs**

In all four mutant *dpy-24* alleles, a significant number of DTCs fail to migrate towards the midbody after reaching the dorsal side and rather move towards the distal ends of the body (Figure 1E and Table 1), indicating that *dpy-24* is important for the directional control of centripetal phase III migration. Previous genetic studies have revealed a role for the netrin pathway in the anterior-posterior axon outgrowth and cell migration (Su et al. 2000a; Levy-Strumpf and Culotti 2007). For instance, overexpression of *unc-40* resulted in the ALM axons to extend in a posterior rather than an anterior direction (Levy-Strumpf and Culotti 2007). Consistently, we found that overexpression of *unc-5* by the *lag-2* promoter caused 16 % of anterior DTCs and 7 % of posterior DTCs to reverse the direction of their centripetal phase III migration (Table 1), revealing a role for *unc-5* in the guidance of phase III DTC migration. Furthermore, in *dpy-24* mutants the DTCs that displayed reversed polarity of centripetal phase III migration showed much brighter *gfp* expression from the transgene *P_{unc-5}:gfp* than those with normal phase III migration (data not shown). These results together suggest that the phase III pathfinding defect of *dpy-24* mutants

may be attributed, at least in part, to *unc-5* overexpression in DTCs. Nevertheless, *dpy-24* also controls the phase III migration direction independent of the netrin pathway since *dpy-24* enhances the phase III pathfinding defect in the *unc-5*, *unc-6*, *unc-40* or *unc-129* null mutant background (Table 2). For instance, the *dpy-24(s71)* and *unc-5(null)* single mutations caused 58% and 6% of anterior DTCs to reverse their phase III migration direction, respectively; however, the *dpy-24(s71); unc-5(null)* double mutations caused significantly higher percentage (98%) of anterior DTCs to display the phase III polarity defect (Table 2). A similar result, but to a lesser extent, was observed in the posterior DTCs. Taken together, *dpy-24* likely controls the polarity of centripetal phase III migration by both *unc-5*-dependent and *unc-5*-independent mechanisms.

Multiple regions of DPY-24 are important for DTC migration

Blimp-1 and PRDI-BF1 have been reported to function as active and passive repressors in different context of target genes. As active repressors, Blimp-1 and PRDI-BF1 repress the transcription of target genes by competing for the same binding sites of transcriptional activators (Keller and Maniatis 1991; Kuo and Calame 2004; Tooze et al. 2006; Doody et al. 2007). However, in the transcription repression of some other target genes, the zinc finger domains of Blimp-1 and PRDI-BF1 appear insufficient and recruiting of co-repressors of the Groucho family of proteins (Ren et al. 1999), histone H3 methyltransferase G9a (Gyory et al. 2004) or histone deacetylase HDAC2 (Yu et al. 2000) is important for transcriptional repression.

The genes *unc-37* and *hda-1* coding for *C. elegans* Groucho and histone deacetylase, respectively, have been shown to be important for gonadogenesis (Miller et al. 1993; Pflugrad et al. 1997; Dufourcq et al. 2002). The worm genome contains at

least 38 genes coding for proteins with a potential SET domain (Andersen and Horvitz 2007). However, none of them have been implicated in DTC migration. The possibility that DPY-24, like Blimp-1 and PRDI-BF1, may function with UNC-37, HDA-1 or SET-domain containing proteins to control DTC migration will need to be further examined.

DPY-24 down-regulation is controlled by heterochronic genes *daf-12*, *dre-1* and *lin-29* to initiate the dorsalward turning of DTCs

Our immunostaining data showed that the disappearance of DPY-24 in DTCs prior to their ventral-to-dorsal phase II turning is regulated by the redundant function of *dre-1*, *lin-29* and, to a lesser extent, *daf-12*. This result suggests two modes of regulation involved in DPY-24 down-regulation, one at the transcriptional level by LIN-29 and DAF-12 and the other at the protein stability level by DRE-1. It is unclear if DPY-24 down-regulation by these three proteins are directly or indirectly. Being a steroid hormone receptor, DAF-12 is likely to repress *dpy-24* transcription indirectly in response to the hormone, on the basis of the general transcription mechanism of steroid hormone receptor. A recent study reveals that the steroid hormone receptor DAF-12 is able to repress gene expression indirectly through transcriptional activation of microRNAs, which in turn bind to the 3' UTR of the target transcripts and result in gene repression (Bethke et al. 2009). *dpy-24* 3' UTR has several microRNA binding sites and these microRNA contains the potential DAF-12 binding sites in their 5' genomic DNA. The involvement of these microRNAs in *dpy-24* down-regulation will need to be investigated. Alternatively, *daf-12* may act through a transcriptional cascade and indirectly control *dpy-24* expression in the DTCs through other transcription factors.

***lin-42* might play as a switch for DTCs making dorsal turns or not.**

It is an interesting issue that why the situation of *dpy-24* suppresses *lin-29* and *daf-12* could be reversed in mid L3 stage. *lin-29* is suppressed by *dpy-24* in early L2 stage, and starts to express from early L3 stage, which indicates the suppression of *dpy-24* to *lin-29* is sort of leaky after early L3. It is probably resulted from the F-Box protein, DRE-1, which is expressed from early L3 to degrade DPY-24.

Hence, *lin-29* could start to accumulate from early L3 and when time goes to mid L3, the level of LIN-29 is then enough to suppress the expression of *dpy-24* in reverse and able to activate *unc-5*. Plus the aid of DRE-1 and DAF-12, *dpy-24* could be completely silenced.

Previous report shows that in *lin-42(RNAi)* mutant, the dorsal turns of DTCs were precociously executed in L2 (Tennessen et al. 2006), which suggests that *lin-42* plays a role to suppress immature dorsal turns like *dpy-24* and might be the top commander in this hierarchy controlling the DTC dorsal migration. The expression pattern of *lin-42* in DTCs has two peaks in L2 and L3 intermolt and disappears in L2 molt and L3 molt. Its disappearance in L3 molt fits the hypothesis that the expression of *lin-42* might be the switch of DTC turns dorsally or not.

We propose that *lin-42* might be the activator of *dpy-24* and the suppressor of *lin-29*. During early L3, the expression of *lin-42* is high, so *dpy-24* is stronger than *lin-29*; while in mid L3, the expression of *lin-42* starts to decline, so *dpy-24* becomes weaker and weaker than *lin-29* (Figure 17). Our preliminary data has proofed that the expression of *dpy-24* in DTCs is precociously be terminated in *lin-42(RNAi)* animals, indicating *lin-42* is a transcriptional activator of *dpy-24*. The relationship between *lin-42* and *lin-29*, maybe *daf-12*, requires further investigation.

UNC5B might be the target of Blimp-1 during lymphocyte chemostasis.

UNC5B is expressed in human immune tissue. The regulation of UNC5B has been proved to play a role during the infiltration of leukocyte (Ly et al. 2005). Our work provides a possibility that Blimp-1 might affect T cell homeostasis through UNC5B. We aligned the promoter sequence of *unc-5* with the regulatory sequence of its mammalian homologue UNC5B and found there are three conserved regions closely located. And interestingly, the two DPY-24 binding sites are in the second conserved box, which suggests that the mammalian homologue of DPY-24, Blimp-1, might directly interact with UNC5B since their binding sequences are almost the same and the similarity between their zinc fingers is up to 87% (Doody et al. 2007).

Therefore, Blimp-1 might inhibit the occurrence of autoimmune disease by suppressing the migration of T cells which is caused by UNC5B and result in over infiltration. It is possible that UNC5B is ectopically expressed in Blimp-1-deficient T cell. Although netrin-1 has been reported to inhibit leukocyte migration, however, UNC5B still has a chance to have other ligands as an alternatives as mentioned in Bruno *et.al.*'s work (Larrivee et al. 2007). Under some stimulation of certain cytokine or growth factor instead of activated by netrin as a ligand, these Blimp-1-deficient T cells caused more wide-spread infiltration and generated colitis as a result (Larrivee et al. 2007).

Evolutionary conservation of DPY-24 and Blimp-1 genes in the control of cell identities during development

Previous studies of Blimp-1 genes in fly, zebrafish and mouse and this work in worm show that Blimp-1 functions as transcription repressor and plays crucial roles in development in multiple species in the animal kingdom. The fly Blimp-1 (dBlimp-1)

controls timing of the ecdysone-induced developmental pathway (Agawa et al. 2007). In zebrafish, Blimp-1 specifies slow-twitch muscle fiber identity in response to hedgehog signaling (Baxendale et al. 2004). The mouse Blimp-1 plays crucial roles in the differentiation and function of B and T lymphocytes (Calame 2008; Martins and Calame 2008) and various epithelial lineages in adult mice including epidermal keratinocytes (Magnusdottir et al. 2007). These studies reveal an evolutionary conserved role of blimp-1 in the control of cell identity during development and specification of cell lineage. Our work in *C. elegans* reveals a previously unassigned function of blimp-1 in the temporal fate determination of migrating cells. In addition, our molecular and genetic work positions *dpy-24* at the end point of the heterochronic circuit and links it directly to the spatial regulator *unc-5*, thus providing a mechanism by which the temporal and spatial signals are coordinated to regulate precise cell migration pattern.



Reference

- Agawa, Y., Sarhan, M., Kageyama, Y., Akagi, K., Takai, M., Hashiyama, K., Wada, T., Handa, H., Iwamatsu, A., Hirose, S. et al. 2007. *Drosophila* Blimp-1 is a transient transcriptional repressor that controls timing of the ecdysone-induced developmental pathway. *Mol Cell Biol* **27**(24): 8739-8747.
- Altun-Gultekin, Z., Andachi, Y., Tsalik, E.L., Pilgrim, D., Kohara, Y., and Hobert, O. 2001. A regulatory cascade of three homeobox genes, *ceh-10*, *ttx-3* and *ceh-23*, controls cell fate specification of a defined interneuron class in *C. elegans*. *Development* **128**(11): 1951-1969.
- Ambros, V. 2000. Control of developmental timing in *Caenorhabditis elegans*. *Curr Opin Genet Dev* **10**(4): 428-433.
- Andersen, E.C. and Horvitz, H.R. 2007. Two *C. elegans* histone methyltransferases repress *lin-3* EGF transcription to inhibit vulval development. *Development* **134**(16): 2991-2999.
- Antebi, A., Norris, C.R., Hedgecock, E.M. and Garriga, G. 1997. Cell and growth cone migrations. *Celegans II* (ed DL Riddle, T Blumenthal, BJ Meyer and JR Priess): pp.583-609.
- Antebi, A., Yeh, W.H., Tait, D., Hedgecock, E.M., and Riddle, D.L. 2000. *daf-12* encodes a nuclear receptor that regulates the dauer diapause and developmental age in *C. elegans*. *Genes Dev* **14**(12): 1512-1527.
- Battye, R., Stevens, A., and Jacobs, J.R. 1999. Axon repulsion from the midline of the *Drosophila* CNS requires slit function. *Development* **126**(11): 2475-2481.
- Baxendale, S., Davison, C., Muxworthy, C., Wolff, C., Ingham, P.W., and Roy, S. 2004. The B-cell maturation factor Blimp-1 specifies vertebrate slow-twitch muscle fiber identity in response to Hedgehog signaling. *Nat Genet* **36**(1):

88-93.

Bethke, A., Fielenbach, N., Wang, Z., Mangelsdorf, D.J., and Antebi, A. 2009. Nuclear hormone receptor regulation of microRNAs controls developmental progression. *Science* **324**(5923): 95-98.

Bettinger, J.C., Lee, K., and Rougvie, A.E. 1996. Stage-specific accumulation of the terminal differentiation factor LIN-29 during *Caenorhabditis elegans* development. *Development* **122**(8): 2517-2527.

Blelloch, R., Anna-Arriola, S.S., Gao, D., Li, Y., Hodgkin, J., and Kimble, J. 1999. The gon-1 gene is required for gonadal morphogenesis in *Caenorhabditis elegans*. *Dev Biol* **216**(1): 382-393.

Blelloch, R. and Kimble, J. 1999. Control of organ shape by a secreted metalloprotease in the nematode *Caenorhabditis elegans*. *Nature* **399**(6736): 586-590.

Brenner, S. 1974. The genetics of *Caenorhabditis elegans*. *Genetics* **77**(1): 71-94.

Calame, K. 2008. Activation-dependent induction of Blimp-1. *Curr Opin Immunol* **20**(3): 259-264.

Chan, S.S., Zheng, H., Su, M.W., Wilk, R., Killeen, M.T., Hedgecock, E.M., and Culotti, J.G. 1996. UNC-40, a *C. elegans* homolog of DCC (Deleted in Colorectal Cancer), is required in motile cells responding to UNC-6 netrin cues. *Cell* **87**(2): 187-195.

Chilton, J.K. 2006. Molecular mechanisms of axon guidance. *Dev Biol* **292**(1): 13-24.

Colavita, A. and Culotti, J.G. 1998. Suppressors of ectopic UNC-5 growth cone steering identify eight genes involved in axon guidance in *Caenorhabditis elegans*. *Dev Biol* **194**(1): 72-85.

Colavita, A., Krishna, S., Zheng, H., Padgett, R.W., and Culotti, J.G. 1998. Pioneer

- axon guidance by UNC-129, a *C. elegans* TGF-beta. *Science* **281**(5377): 706-709.
- Crowner, D., Madden, K., Goeke, S., and Giniger, E. 2002. Lola regulates midline crossing of CNS axons in *Drosophila*. *Development* **129**(6): 1317-1325.
- Culotti, J.G. and Merz, D.C. 1998. DCC and netrins. *Curr Opin Cell Biol* **10**(5): 609-613.
- Doody, G.M., Stephenson, S., McManamy, C., and Tooze, R.M. 2007. PRDM1/BLIMP-1 modulates IFN-gamma-dependent control of the MHC class I antigen-processing and peptide-loading pathway. *J Immunol* **179**(11): 7614-7623.
- Drescher, U., Kremoser, C., Handwerker, C., Loschinger, J., Noda, M., and Bonhoeffer, F. 1995. In vitro guidance of retinal ganglion cell axons by RAGS, a 25 kDa tectal protein related to ligands for Eph receptor tyrosine kinases. *Cell* **82**(3): 359-370.
- Dufourcq, P., Victor, M., Gay, F., Calvo, D., Hodgkin, J., and Shi, Y. 2002. Functional requirement for histone deacetylase 1 in *Caenorhabditis elegans* gonadogenesis. *Mol Cell Biol* **22**(9): 3024-3034.
- Eickholt, B.J. 2008. Functional diversity and mechanisms of action of the semaphorins. *Development* **135**(16): 2689-2694.
- Fielenbach, N. and Antebi, A. 2008. *C. elegans* dauer formation and the molecular basis of plasticity. *Genes Dev* **22**(16): 2149-2165.
- Fielenbach, N., Guardavaccaro, D., Neubert, K., Chan, T., Li, D., Feng, Q., Hutter, H., Pagano, M., and Antebi, A. 2007. DRE-1: an evolutionarily conserved F box protein that regulates *C. elegans* developmental age. *Dev Cell* **12**(3): 443-455.
- Finney, M. and Ruvkun, G. 1990. The unc-86 gene product couples cell lineage and

- cell identity in *C. elegans*. *Cell* **63**(5): 895-905.
- Fradkin, L.G., Noordermeer, J.N., and Nusse, R. 1995. The *Drosophila* Wnt protein DWnt-3 is a secreted glycoprotein localized on the axon tracts of the embryonic CNS. *Dev Biol* **168**(1): 202-213.
- Ghosh, N., Gyory, I., Wright, G., Wood, J., and Wright, K.L. 2001. Positive regulatory domain I binding factor 1 silences class II transactivator expression in multiple myeloma cells. *J Biol Chem* **276**(18): 15264-15268.
- Gyory, I., Wu, J., Fejer, G., Seto, E., and Wright, K.L. 2004. PRDI-BF1 recruits the histone H3 methyltransferase G9a in transcriptional silencing. *Nat Immunol* **5**(3): 299-308. Epub 2004 Feb 22.
- Hedgecock, E.M., Culotti, J.G., and Hall, D.H. 1990a. The *unc-5*, *unc-6*, and *unc-40* genes guide circumferential migrations of pioneer axons and mesodermal cells on the epidermis in *C. elegans*. *Neuron* **4**(1): 61-85.
- Hedgecock, E.M., Culotti, J.G., and Hall, D.H. 1990b. The *unc-5*, *unc-6*, and *unc-40* genes guide circumferential migrations of pioneer axons and mesodermal cells on the epidermis in *C. elegans*. *Neuron* **4**(1): 61-85.
- Hedgecock, E.M., Culotti, J.G., Hall, D.H., and Stern, B.D. 1987. Genetics of cell and axon migrations in *Caenorhabditis elegans*. *Development* **100**(3): 365-382.
- Hirai, H., Maru, Y., Hagiwara, K., Nishida, J., and Takaku, F. 1987. A novel putative tyrosine kinase receptor encoded by the *eph* gene. *Science* **238**(4834): 1717-1720.
- Huang, S., Shao, G., and Liu, L. 1998. The PR domain of the Rb-binding zinc finger protein RIZ1 is a protein binding interface and is related to the SET domain functioning in chromatin-mediated gene expression. *J Biol Chem* **273**(26): 15933-15939.

- Ishii, N., Wadsworth, W.G., Stern, B.D., Culotti, J.G., and Hedgecock, E.M. 1992. UNC-6, a laminin-related protein, guides cell and pioneer axon migrations in *C. elegans*. *Neuron* **9**(5): 873-881.
- Jeon, M., Gardner, H.F., Miller, E.A., Deshler, J., and Rougvie, A.E. 1999. Similarity of the *C. elegans* developmental timing protein LIN-42 to circadian rhythm proteins. *Science* **286**(5442): 1141-1146.
- Kamath, R.S., Martinez-Campos, M., Zipperlen, P., Fraser, A.G., and Ahringer, J. 2001. Effectiveness of specific RNA-mediated interference through ingested double-stranded RNA in *Caenorhabditis elegans*. *Genome Biol* **2**(1): RESEARCH0002.
- Keller, A.D. and Maniatis, T. 1991. Identification and characterization of a novel repressor of beta-interferon gene expression. *Genes Dev* **5**(5): 868-879.
- Kidd, T., Bland, K.S., and Goodman, C.S. 1999. Slit is the midline repellent for the robo receptor in *Drosophila*. *Cell* **96**(6): 785-794.
- Killeen, M.T. and Sybingco, S.S. 2008. Netrin, Slit and Wnt receptors allow axons to choose the axis of migration. *Dev Biol* **323**(2): 143-151.
- Kimble, J. and Hirsh, D. 1979. The postembryonic cell lineages of the hermaphrodite and male gonads in *Caenorhabditis elegans*. *Dev Biol* **70**(2): 396-417.
- Kouzarides, T. 2002. Histone methylation in transcriptional control. *Curr Opin Genet Dev* **12**(2): 198-209.
- Kuo, T.C. and Calame, K.L. 2004. B lymphocyte-induced maturation protein (Blimp)-1, IFN regulatory factor (IRF)-1, and IRF-2 can bind to the same regulatory sites. *J Immunol* **173**(9): 5556-5563.
- Labrador, J.P., O'Keefe, D., Yoshikawa, S., McKinnon, R.D., Thomas, J.B., and Bashaw, G.J. 2005. The homeobox transcription factor even-skipped regulates

- netrin-receptor expression to control dorsal motor-axon projections in *Drosophila*. *Curr Biol* **15**(15): 1413-1419.
- Larrivee, B., Freitas, C., Trombe, M., Lv, X., Delafarge, B., Yuan, L., Bouvree, K., Breant, C., Del Toro, R., Brechot, N. et al. 2007. Activation of the UNC5B receptor by Netrin-1 inhibits sprouting angiogenesis. *Genes Dev* **21**(19): 2433-2447.
- Lehmann, R. 2001. Cell migration in invertebrates: clues from border and distal tip cells. *Curr Opin Genet Dev* **11**(4): 457-463.
- Leung-Hagesteijn, C., Spence, A.M., Stern, B.D., Zhou, Y., Su, M.W., Hedgecock, E.M., and Culotti, J.G. 1992. UNC-5, a transmembrane protein with immunoglobulin and thrombospondin type 1 domains, guides cell and pioneer axon migrations in *C. elegans*. *Cell* **71**(2): 289-299.
- Levy-Strumpf, N. and Culotti, J.G. 2007. VAB-8, UNC-73 and MIG-2 regulate axon polarity and cell migration functions of UNC-40 in *C. elegans*. *Nat Neurosci* **10**(2): 161-168.
- Lin, Y., Wong, K., and Calame, K. 1997. Repression of c-myc transcription by Blimp-1, an inducer of terminal B cell differentiation. *Science* **276**(5312): 596-599.
- Ludewig, A.H., Kober-Eisermann, C., Weitzel, C., Bethke, A., Neubert, K., Gerisch, B., Hutter, H., and Antebi, A. 2004. A novel nuclear receptor/coregulator complex controls *C. elegans* lipid metabolism, larval development, and aging. *Genes Dev* **18**(17): 2120-2133.
- Ly, N.P., Komatsuzaki, K., Fraser, I.P., Tseng, A.A., Prodhan, P., Moore, K.J., and Kinane, T.B. 2005. Netrin-1 inhibits leukocyte migration in vitro and in vivo. *Proc Natl Acad Sci U S A* **102**(41): 14729-14734.

- MacNeil, L.T., Hardy, W.R., Pawson, T., Wrana, J.L., and Culotti, J.G. 2009. UNC-129 regulates the balance between UNC-40 dependent and independent UNC-5 signaling pathways. *Nat Neurosci* **12**(2): 150-155.
- Magnusdottir, E., Kalachikov, S., Mizukoshi, K., Savitsky, D., Ishida-Yamamoto, A., Panteleyev, A.A., and Calame, K. 2007. Epidermal terminal differentiation depends on B lymphocyte-induced maturation protein-1. *Proc Natl Acad Sci U S A* **104**(38): 14988-14993.
- Maloof, J.N., Whangbo, J., Harris, J.M., Jongeward, G.D., and Kenyon, C. 1999. A Wnt signaling pathway controls hox gene expression and neuroblast migration in *C. elegans*. *Development* **126**(1): 37-49.
- Martins, G. and Calame, K. 2008. Regulation and functions of Blimp-1 in T and B lymphocytes. *Annu Rev Immunol* **26**: 133-169.
- Miller, D.M., 3rd, Niemeyer, C.J., and Chitkara, P. 1993. Dominant *unc-37* mutations suppress the movement defect of a homeodomain mutation in *unc-4*, a neural specificity gene in *Caenorhabditis elegans*. *Genetics* **135**(3): 741-753.
- Montell, D.J. 1999. The genetics of cell migration in *Drosophila melanogaster* and *Caenorhabditis elegans* development. *Development* **126**(14): 3035-3046.
- Nash, B., Colavita, A., Zheng, H., Roy, P.J., and Culotti, J.G. 2000. The forkhead transcription factor UNC-130 is required for the graded spatial expression of the UNC-129 TGF-beta guidance factor in *C. elegans*. *Genes Dev* **14**(19): 2486-2500.
- Nishiwaki, K., Kubota, Y., Chigira, Y., Roy, S.K., Suzuki, M., Schvarzstein, M., Jigami, Y., Hisamoto, N., and Matsumoto, K. 2004. An NDPase links ADAM protease glycosylation with organ morphogenesis in *C. elegans*. *Nat Cell Biol* **6**(1): 31-37.

- Okada, A., Charron, F., Morin, S., Shin, D.S., Wong, K., Fabre, P.J., Tessier-Lavigne, M., and McConnell, S.K. 2006. Boc is a receptor for sonic hedgehog in the guidance of commissural axons. *Nature* **444**(7117): 369-373.
- Perrone, C.A., Yang, P., O'Toole, E., Sale, W.S., and Porter, M.E. 1998. The *Chlamydomonas* IDA7 locus encodes a 140-kDa dynein intermediate chain required to assemble the II inner arm complex. *Mol Biol Cell* **9**(12): 3351-3365.
- Pflugrad, A., Meir, J.Y., Barnes, T.M., and Miller, D.M., 3rd. 1997. The Groucho-like transcription factor UNC-37 functions with the neural specificity gene *unc-4* to govern motor neuron identity in *C. elegans*. *Development* **124**(9): 1699-1709.
- Piskurich, J.F., Lin, K.I., Lin, Y., Wang, Y., Ting, J.P., and Calame, K. 2000. BLIMP-1 mediates extinction of major histocompatibility class II transactivator expression in plasma cells. *Nat Immunol* **1**(6): 526-532.
- Ren, B., Chee, K.J., Kim, T.H., and Maniatis, T. 1999. PRDI-BF1/Blimp-1 repression is mediated by corepressors of the Groucho family of proteins. *Genes Dev* **13**(1): 125-137.
- Rothberg, J.M., Jacobs, J.R., Goodman, C.S., and Artavanis-Tsakonas, S. 1990. slit: an extracellular protein necessary for development of midline glia and commissural axon pathways contains both EGF and LRR domains. *Genes Dev* **4**(12A): 2169-2187.
- Rowse-Eagle, D., Watson, H.D., and Tignor, G.H. 1981. Improved method for trypsin digestion of Paraplast sections before immunofluorescence staining. *J Clin Microbiol* **13**(5): 996-997.
- Seeger, M., Tear, G., Ferres-Marco, D., and Goodman, C.S. 1993. Mutations affecting

growth cone guidance in *Drosophila*: genes necessary for guidance toward or away from the midline. *Neuron* **10**(3): 409-426.

Shostak, Y., Van Gilst, M.R., Antebi, A., and Yamamoto, K.R. 2004. Identification of *C. elegans* DAF-12-binding sites, response elements, and target genes. *Genes Dev* **18**(20): 2529-2544.

Su, M., Merz, D.C., Killeen, M.T., Zhou, Y., Zheng, H., Kramer, J.M., Hedgecock, E.M., and Culotti, J.G. 2000a. Regulation of the UNC-5 netrin receptor initiates the first reorientation of migrating distal tip cells in *Caenorhabditis elegans*. *Development* **127**(3): 585-594.

Su, M., Merz, D.C., Killeen, M.T., Zhou, Y., Zheng, H., Kramer, J.M., Hedgecock, E.M., and Culotti, J.G. 2000b. Regulation of the UNC-5 netrin receptor initiates the first reorientation of migrating distal tip cells in *Caenorhabditis elegans*. *Development* **127**(3): 585-594.

Sulston, J.E. and Horvitz, H.R. 1977. Post-embryonic cell lineages of the nematode, *Caenorhabditis elegans*. *Dev Biol* **56**(1): 110-156.

Sulston, J.E.a.H., J. 1988. The Nematode *Caenorhabditis elegans* Methods. *Cold Spring Harbor Laboratory Press*.

Tamai, K.K. and Nishiwaki, K. 2007. bHLH transcription factors regulate organ morphogenesis via activation of an ADAMTS protease in *C. elegans*. *Dev Biol* **308**(2): 562-571.

Tennessen, J.M., Gardner, H.F., Volk, M.L., and Rougvie, A.E. 2006. Novel heterochronic functions of the *Caenorhabditis elegans* period-related protein LIN-42. *Dev Biol* **289**(1): 30-43.

Tooze, R.M., Stephenson, S., and Doody, G.M. 2006. Repression of IFN-gamma induction of class II transactivator: a role for PRDM1/Blimp-1 in regulation of

- cytokine signaling. *J Immunol* **177**(7): 4584-4593.
- Turner, C.A., Jr., Mack, D.H., and Davis, M.M. 1994. Blimp-1, a novel zinc finger-containing protein that can drive the maturation of B lymphocytes into immunoglobulin-secreting cells. *Cell* **77**(2): 297-306.
- Wadsworth, W.G., Bhatt, H., and Hedgecock, E.M. 1996. Neuroglia and pioneer neurons express UNC-6 to provide global and local netrin cues for guiding migrations in *C. elegans*. *Neuron* **16**(1): 35-46.
- Whangbo, J. and Kenyon, C. 1999. A Wnt signaling system that specifies two patterns of cell migration in *C. elegans*. *Mol Cell* **4**(5): 851-858.
- Wicks, S.R., Yeh, R.T., Gish, W.R., Waterston, R.H., and Plasterk, R.H. 2001. Rapid gene mapping in *Caenorhabditis elegans* using a high density polymorphism map. *Nat Genet* **28**(2): 160-164.
- Williams, B.D., Schrank, B., Huynh, C., Shownkeen, R., and Waterston, R.H. 1992. A genetic mapping system in *Caenorhabditis elegans* based on polymorphic sequence-tagged sites. *Genetics* **131**(3): 609-624.
- Wu, Y.C., Cheng, T.W., Lee, M.C., and Weng, N.Y. 2002. Distinct rac activation pathways control *Caenorhabditis elegans* cell migration and axon outgrowth. *Dev Biol* **250**(1): 145-155.
- Yu, J., Angelin-Duclos, C., Greenwood, J., Liao, J., and Calame, K. 2000. Transcriptional repression by blimp-1 (PRDI-BF1) involves recruitment of histone deacetylase. *Mol Cell Biol* **20**(7): 2592-2603.

Figures and Tables

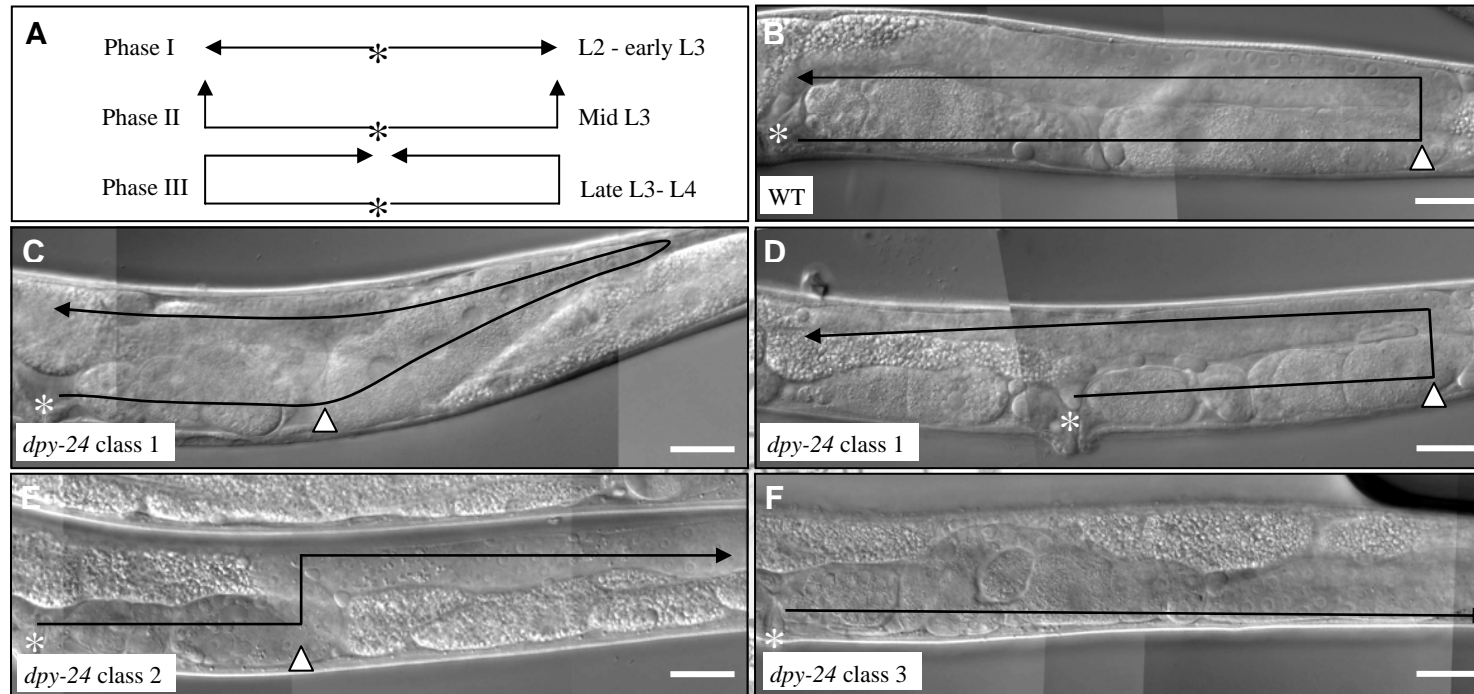


Figure 1. DTC migration defects in *dpy-24* mutants. (A) Diagrams show the three phases of DTC migration. Arrowheads indicate DTCs, while asterisks indicate the position of vulva. (B) Normal gonad in N2 wild type; (C, D) Class 1 defect of gonad in *dpy-24* mutant with precocious dorsal turn; (E) Class 2 defect of gonad in *dpy-24* mutant with precocious dorsal turn and abnormal phase III migration; (F) Class 3 defect of gonad in *dpy-24* mutant with neither dorsal turn nor centripetal turn. Black lines indicate the DTC migrating path and the black arrowheads point out the direction of DTC migration, while the blank arrowheads point out the site of dorsal turn. The blank asterisks mark the vulva. Scale bar 40 μ m.

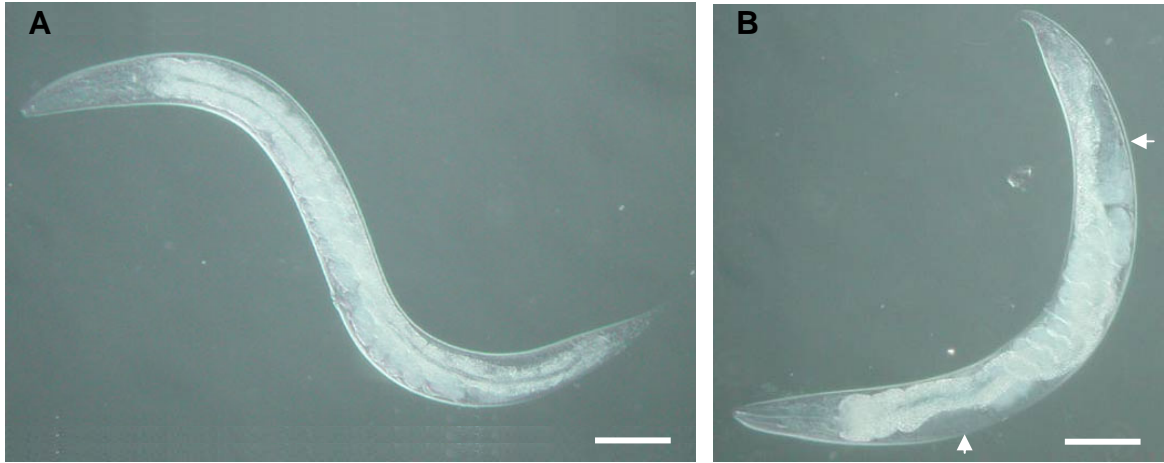
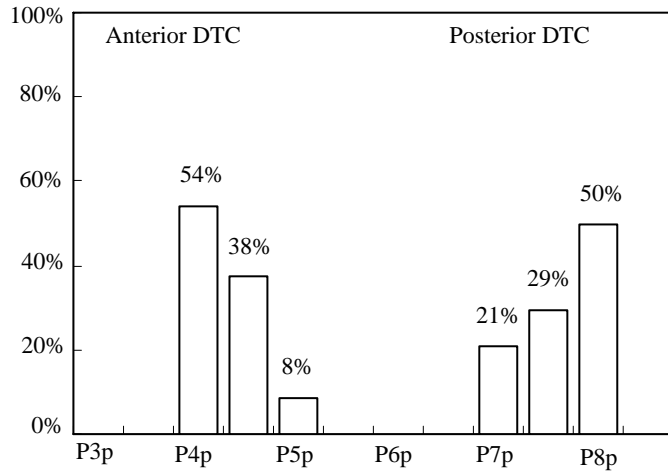


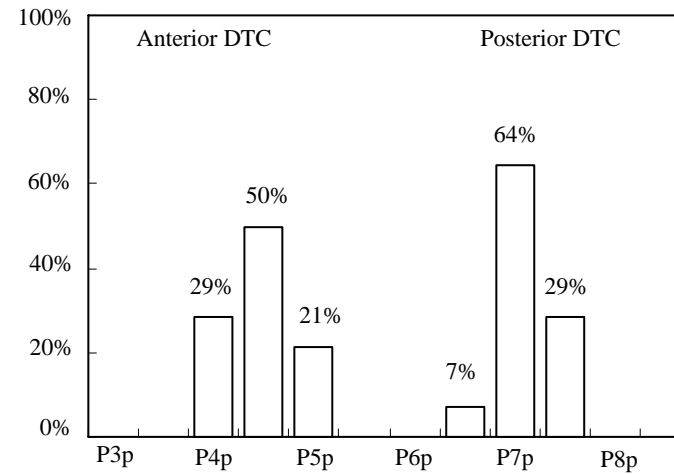
Figure 2. *dpy-24* mutant exhibits white patches under dissecting microscope. (A) N2 wild-type; (B) *dpy-24(s71)*. A and B show the difference of body length and slimness between WT and *dpy-24*. The arrows indicate the white patches in *dpy-24* which are caused by aberrant DTC migration. Scale bar 100 μ m.



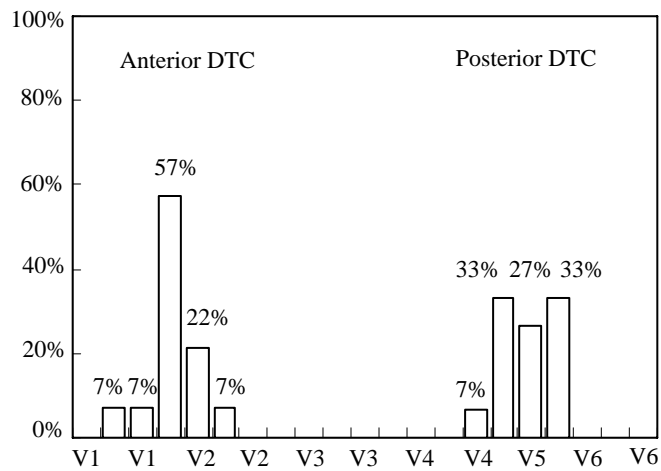
N2 at L2 molt (1 cell stage)



***dpy-24* at L2 molt (1 cell stage)**



N2 at mid L3 (2 cell stage)



***dpy-24* at mid L3 (2 cell stage)**

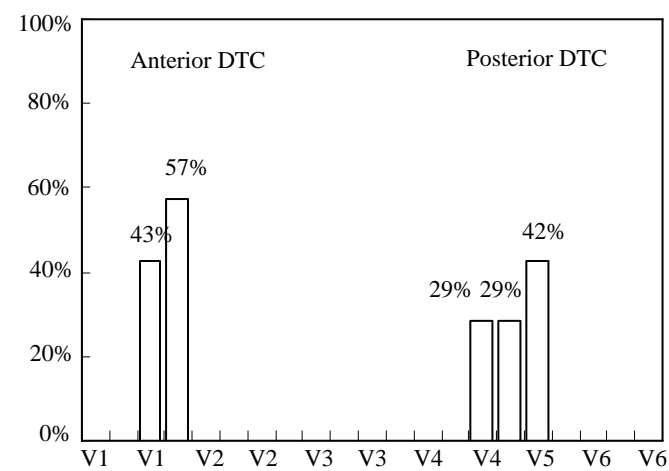


Figure 3. The migration speed of DTC in *dpy-24* mutant is similar to that in N2 wild type.

Figure 3. The migration speed of DTC in *dpy-24* mutant is similar to that in N2 wild type. Diagrams show the percentages of anterior and posterior DTC in N2 and *dpy-24* mutant reaching specific cell landmark in early L2 molt and mid L3 stage. Vn (n=1,2,3,4 and 6) is the abbreviation of Vn.papp and Vn.pppp and V5 is the abbreviation of V5.pppp.



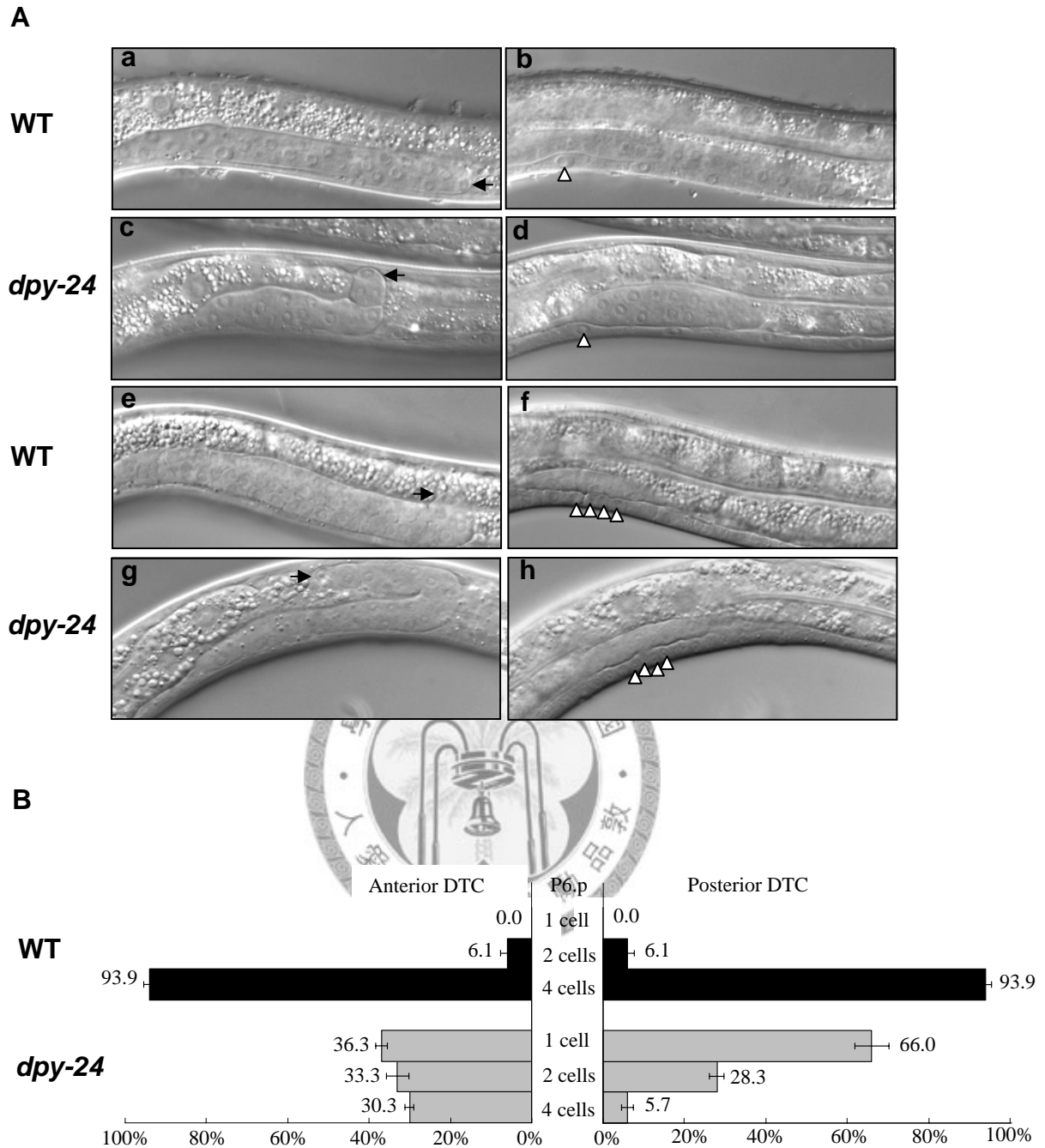


Figure 4. DTC makes a precocious dorsal turn in *dpy-24* mutant. (A) (a-d) In early L3 stage (P6.p 1-cell), DTC in N2 remains not turning dorsally, while DTC in *dpy-24* mutant has made its dorsal turn. (e-h) In late L3 stage (P6.p 4-cell), while DTC in N2 just made it dorsal turn, DTC in *dpy-24* mutant has reached the halfway of its phase III centripetal migration. Arrows indicate DTC and the blank arrowheads indicate the lineage of P6.p. (B) Diagram shows the percentage of in which P6.p lineage stage the anterior and posterior DTC in N2 and *dpy-24* mutant made its dorsal turn.

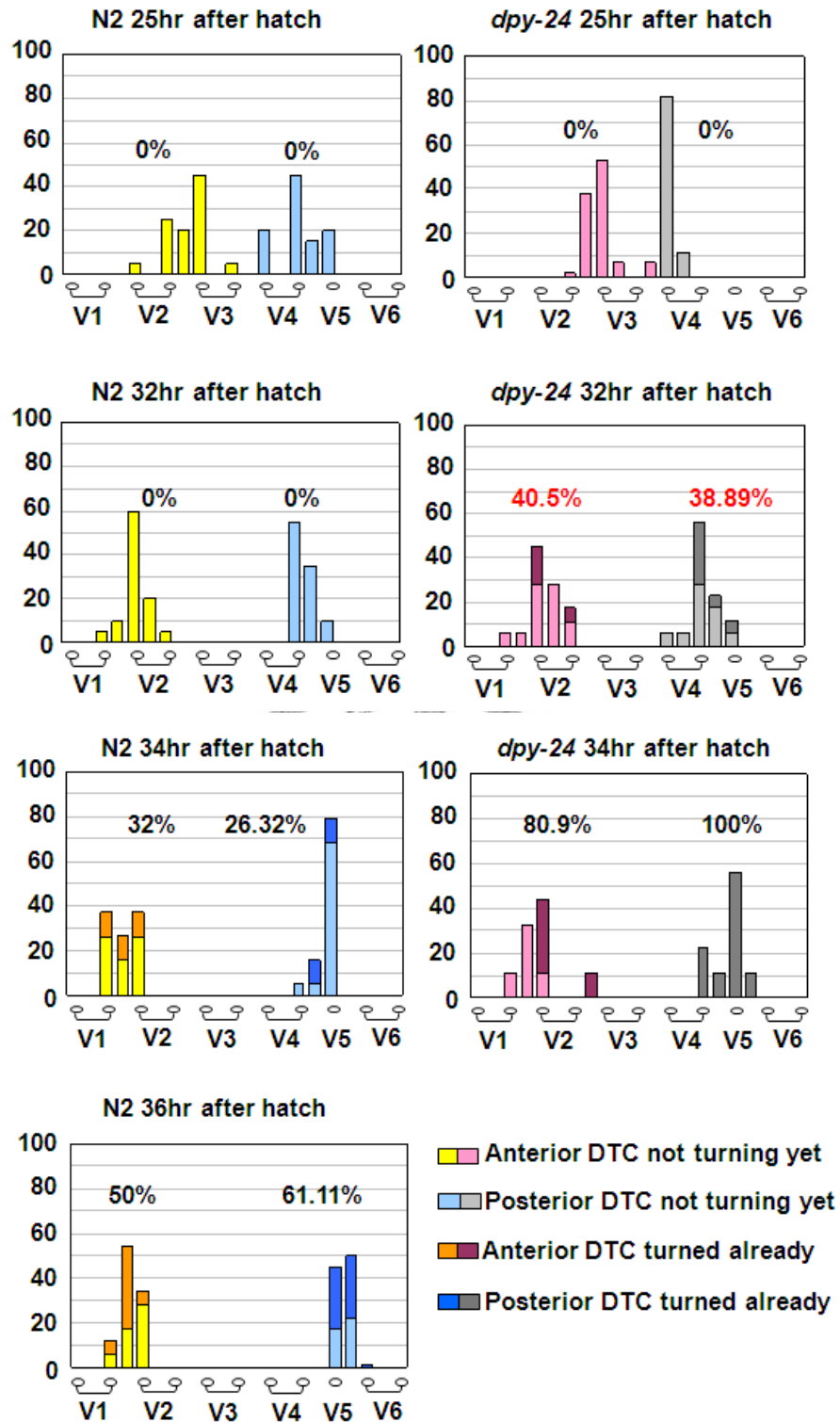


Figure 5. DTC makes its dorsal turn 3.5 hr earlier in *dpy-24* mutant than in N2 wild type. The X axis indicates the position of the hypodermal V cells. The lower-left panel shows the colors corresponding DTCs which turned dorsally already or not turned dorsally yet, and the Y axis indicates the percentage of DTCs in different colors respectively. The percentages labeled in the diagrams indicate the percentages of turned DTC.

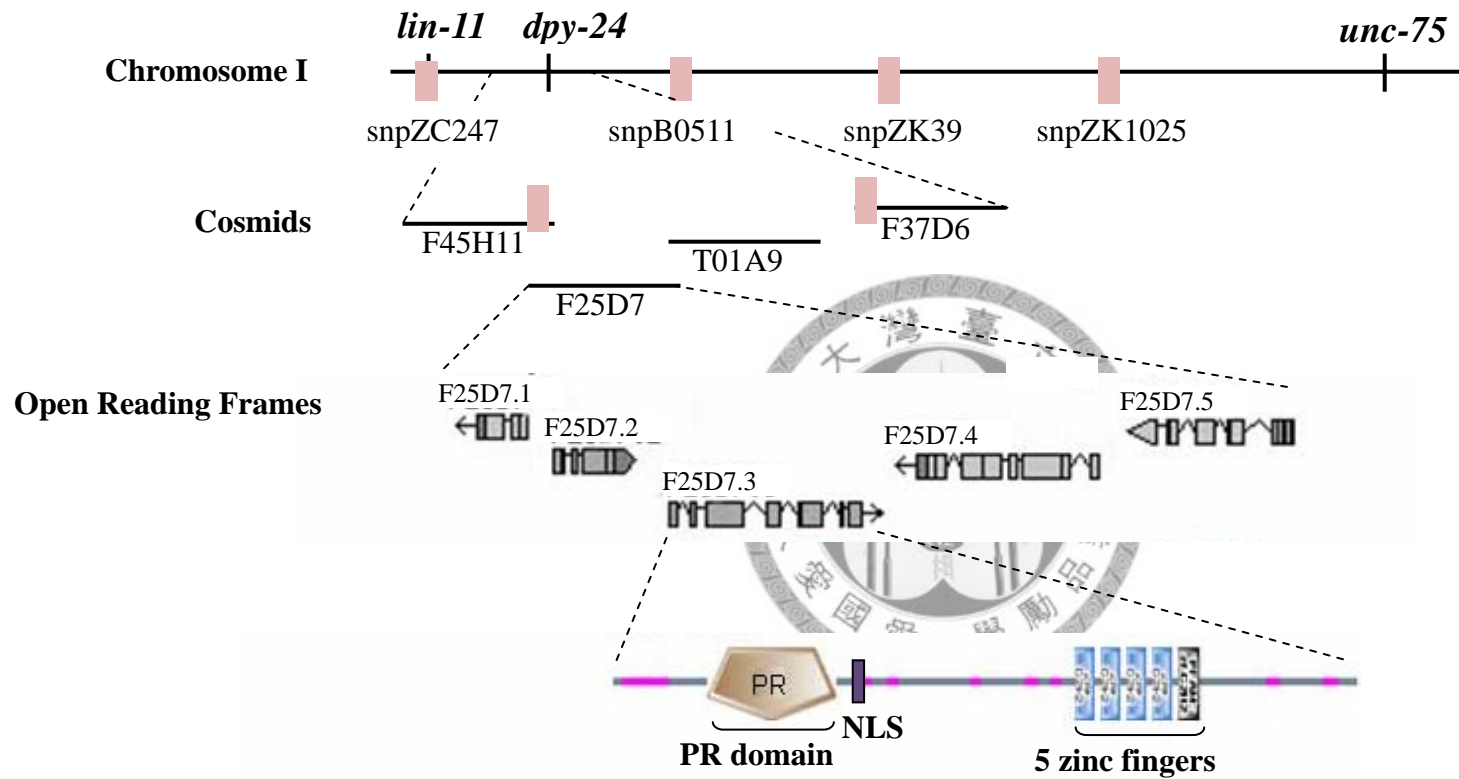
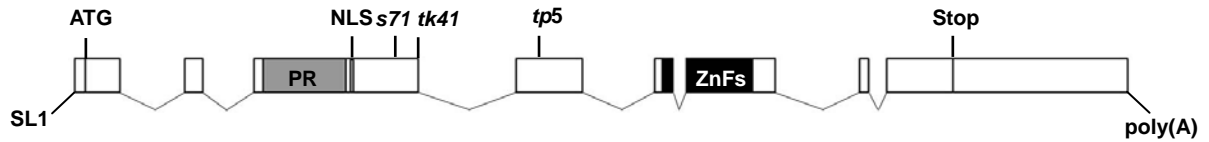


Figure 6. The genetic mapping and molecular cloning of *dpy-24*.

A



B

DPY-24	1	M-----GQSGDGDGVPAPFSSAAAAAHSPPHSPLSVGVSSASSATSSSSSTPPSSTSPAGVVSASGARNVTDWKQS
Blimp-1	1	MRAYLRWIFSWKNVWVRPCQRLHFKTVLQGSLLYLTALDSYSVQAAKSSSSGSVKFQGLAETGIMKMDMEDADMTLW
PRDI-BF1	1	M-----KMDMEDADMTLW
DPY-24	72	GQENLAQLCIHVPDK----SVSLPNPKRACTLPNLLILSSSK-NRKKSSLWSSDHIPIRGVRFGLVGEIRLVDVDTA
Blimp-1	81	TEAEFEKCTYLVNDHPWDSGADGGTSVQAEASLPRNLLFYAANNSKEVIGVVSKEYIPKGTFRFGPLIGEVYINDTVPK
PRDI-BF1	14	TEAEFEKCTYLVNDHPWDSGADGGTSVQAEASLPRNLLFYATN-SEEVIGVMSKEYIPKGTFRFGPLIGEVYINDTVPK
DPY-24	147	LVCPAEASMAGGGPAQEDVPFDEAPEEKKIYSPSGRLNKTICVKDDARSNWVKYVAAEEDFQNLVAACIQNDIYFYT
Blimp-1	161	NAN-----RKYFWRIYSR--BEFHHEIDGFNEEKSNWVRVYVNPASAREQNLAAQNGMNIYFYT
PRDI-BF1	93	NAN-----RKYFWRIYSR--GELHHEIDGFNEEKSNWVRVYVNPASAREQNLAAQNGMNIYFYT
		s71 (STOP)
DPY-24	227	VKLEANTELSPWESRDYARKLNYSTRPYVVRVRRPQATQLIPSPAPPASATAIASLAETIIVADIVSVKLLIESPIDTLSTD
Blimp-1	219	IKFIPANQELLVWYCRDFAERDHYPPYGELTVLN--LTQTSNPKQYSSEKNELYPKSVPKREYSVKEILKLDNPSKPK
PRDI-BF1	151	IKFIPANQELLVWYCRDFAERDHYPPYGELTMN--LTQTSNPKQYSSEKNELCPKNVPKREYSVKEILKLDNPSKPK
DPY-24	307	ASSASDEEMDVEEQESCTR-----FVAEVTFRNVIQNPV
Blimp-1	297	DHYRSNISPTLTKDMDGFRKNGSPDMPFYPRVYPIRAPLPEDFLKASLAYGERPTYITHSPSPSSSTPSPASSSPE
PRDI-BF1	229	DHYRSNISPTLTKDMDGFRKNGSPDMPFYPRVYPIRAPLPEDFLKASLAYGERPTYITRSPSPSSSTPSPARSSPD
		tk41 (STOP)
DPY-24	342	VRPVAQKVNPFPGIPVRLGNFYASPLVDFKEFMRKSLQKLVDSMFVSPVAQTAAITAAGGRSGQPIDVQVLAATAG
Blimp-1	377	QSLKSSSPHSSPGNTVSPVPLAPLPEHRDYSYLNVSYGSEGLGSPGYAPAPHLPPAFIPSYNAHYPKFLLPYGTSSNG
PRDI-BF1	309	QSLKSSSPHSSPGNTVSPVPGSQEHRDYSYALNASYGTGLGSPGYAPAPHLPPAFIPSYNAHYPKFLLPYGMNCNG
		tp5 (STOP)
DPY-24	422	AHFGN-----YAAVYGSQDFQHEHESKPF-----FYTSASAPAGGGGCMC-
Blimp-1	457	LSTMNNNGINNFSLFPRLYPVYSNLLSGSLPHEMLNPASLPSLPTDGARRLLQPEHPREVLPAPHSAPSLTCAAS
PRDI-BF1	389	LSAVSSNGINNFGLFPRLCPVYSNLLGGGSLPHEMLNPASLPSLPSDGARRLLQPEHPREVLPAPHSAPSLTCAAS
DPY-24	460	-----GGFGMGSAHTSSFHQLFVN--HSSSSHNDSSFNQVFN-----YVQQQENGKTRVYACKDCNKTF
Blimp-1	537	MKDES-SPPSGSPTAGTAATSEHVVOPKATSSVMAAPSTDGAMNLIKKNRNMGTGKTLPLKKNQNGKIRYECNVCAKTF
PRDI-BF1	469	MKDKACSPTSPTSAGTAATAEHVVOPKATSAAMAAPSSDEAMNLIKKNRNMGTGKTLPLKKNQNGKIRYECNVCAKTF
		oooooooooooo
DPY-24	518	GQLSNLKVHVRHTGERPFKCEICNKEFTQLAHLQKHHLVHTGERPHERCDICDKRFSSTSNLKTHLRLHNGOKPYTCQVC
Blimp-1	616	GQLSNLKVHVRVHSGERPFKCEICNKEFTQLAHLQKHHLVHTGERPHERCQVCHKRFSSSTSNLKTHLRLHSGEKPYQCKVC
PRDI-BF1	549	GQLSNLKVHVRVHSGERPFKCEICNKEFTQLAHLQKHHLVHTGERPHERCQVCHKRFSSSTSNLKTHLRLHSGEKPYQCKVC
		oooooooooooo ooo
DPY-24	598	DAKFTQVHLRHLKRLHANERPYSCTCGKRYISPSGLRTEHWKTTTCKEEDMKDSMRDDIMDKGEIDEGSMSGSYGNL
Blimp-1	696	PAKFTQVHLRHLKRLHTRERPHKCAQCHRSYIHLCSLKVLEKGNCPACPAAGLPLEDLTRINEIERFDISDN----
PRDI-BF1	629	PAKFTQVHLRHLKRLHTRERPHKCAQCHRSYIHLCSLKVLEKGNCAAAPAGLPLEDLTRINEIERFDISDN----
		oooooooooooo ooo
DPY-24	678	GIFENTLNSLKRPLMPHETIISKYINPNASDLGQGPSGMOEQQAPPPTSQQQOHMMYQNTMGHGQGSHTQGP PPPQH
Blimp-1	770	-----ADRLDMEDSVDVTSMVEKEILAVVR--KEKEETSLKVSQORNMGN-----LLSSGCSLYE-----
PRDI-BF1	703	-----ADRLDMEDSVDVTSMVEKEILAVVR--KEKEETGLKVSQORNMGN-----LLSSGCSLYE-----
DPY-24	758	FQMDHSGMQNGGGIPHQHQLIQGGPSSGSGQQQHPOHNGIHRLPDKNPLPVLGLPHYP
Blimp-1	825	-----SSDLSLMLKLPSSN---PLPLVPVKVQETVEPMDP
PRDI-BF1	758	-----SSDLPMLKLPSSN---PLPLVPVKVQETVEPMDP

Figure 7. The *dpy-24* gene and protein. (A) The gene structure of *dpy-24* indicating different allele mutation sites and regions corresponding to encode PR, NLS and Zinc fingers domains. (B) Alignment among the protein sequence of DPY-24, PRDI-BF1 and Blimp-1. Black and light grey box-shaded indicate identical residues, dark grey box-shaded indicate similar residues. Black lines beneath highlight the region of PR domain and the circles beneath describe the region of zinc fingers. The boxed residues are the signal of nuclear localization. The mutation sites of different alleles are pointed out by the black arrowheads.

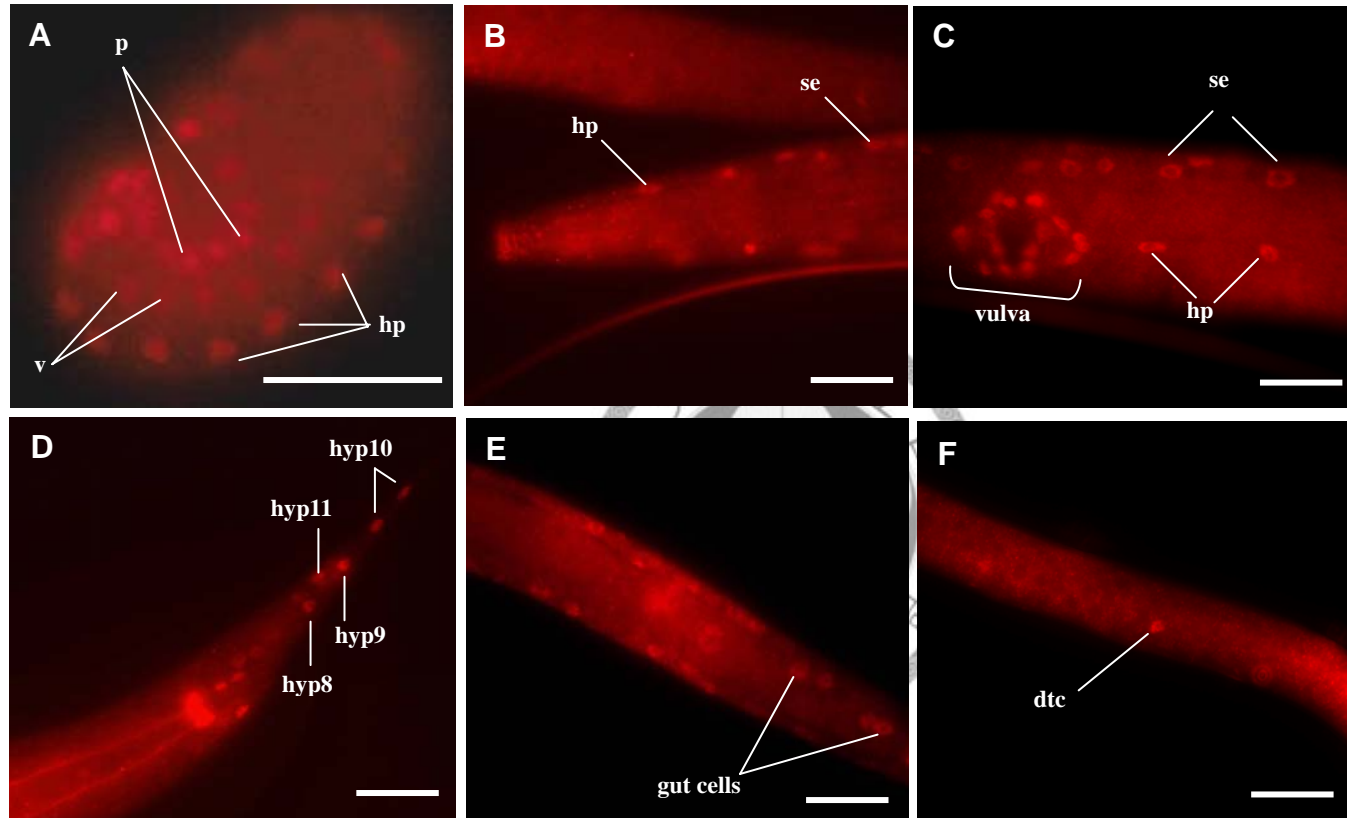


Figure 8. Dpy-24 expression pattern. Anti-DPY-24 antibody staining of wild-type embryo (A) and larvae (B-F). (A) DPY-24 was detected in hyp7 (hp), V cells (v) and P cell precursors (p) in a 1.5 fold embryo. (B-E) DPY-24 is expressed in hypodermal cells (hp), seam cells (se) (B and C), vulval cells (C), gut cells (E), hyp8-hyp11 (D). (F) DPY-24 was detected in the DTC at the L2 stage. Scale bars are 40 μ m.

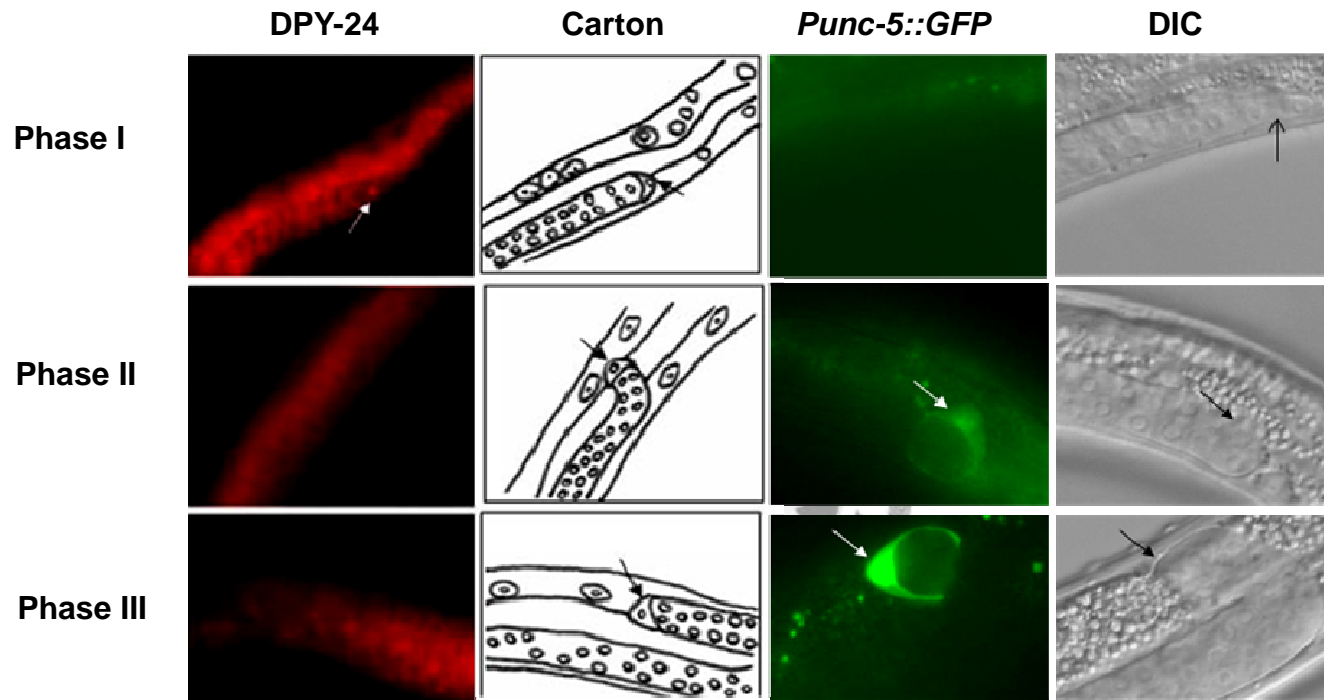


Figure 9. DPY-24 expression is transient in the first phase of DTC migration, and its expression is complementary to *unc-5* expression. Arrows indicate DTC.

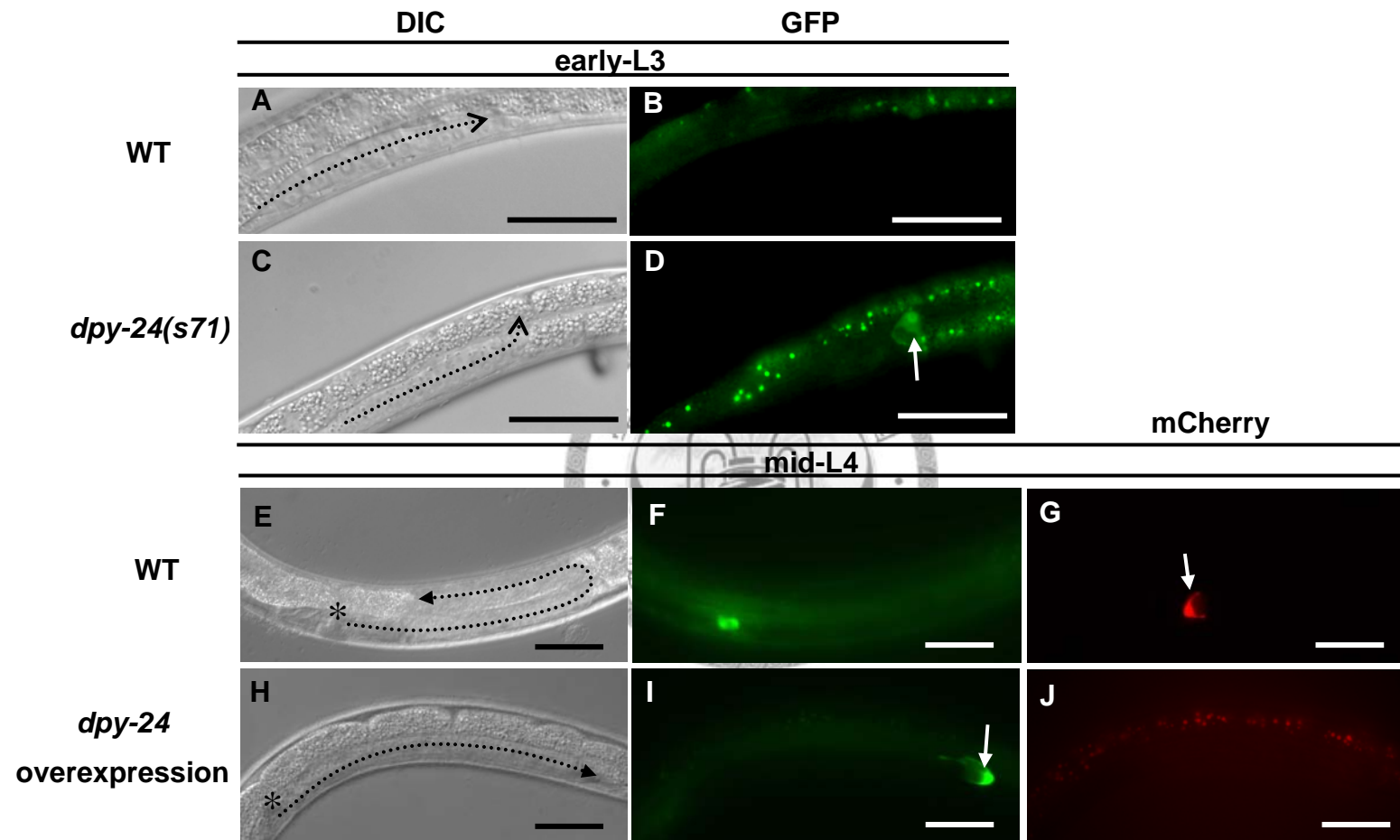
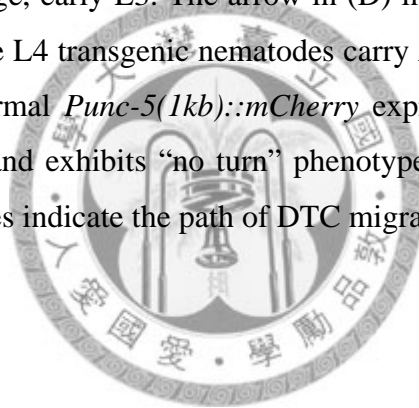


Figure 10. *unc-5* is precociously activated in *dpy-24* mutant and is suppressed when *dpy-24* is ectopically expressed.

Figure 10. *unc-5* is precociously activated in *dpy-24* mutant and is suppressed when *dpy-24* is ectopically expressed. (A-D) N2 (A,B) and *dpy-24* (C,D) are at the same larval developmental stage, early L3. The arrow in (D) indicating the precocious *Punc-5::gfp* expression in DTC with early dorsal migration in *dpy-24* mutant. (E-J) The L4 transgenic nematodes carry *Pdpy-24::dpy-24::gfp* and *Punc-5(1kb)::mCherry*. (E-G) DTC without DPY-24GFP ectopic expression has normal *Punc-5(1kb)::mCherry* expression, while in (H-J) DTC with ectopic DPY-24GFP expression has no *Punc-5(1kb)::mCherry* expression and exhibits “no turn” phenotype. The asterisks indicate the developmental stage of the vulva and the white arrow indicates DTC. The dash lines indicate the path of DTC migration. Scale bars are 40 μ m.



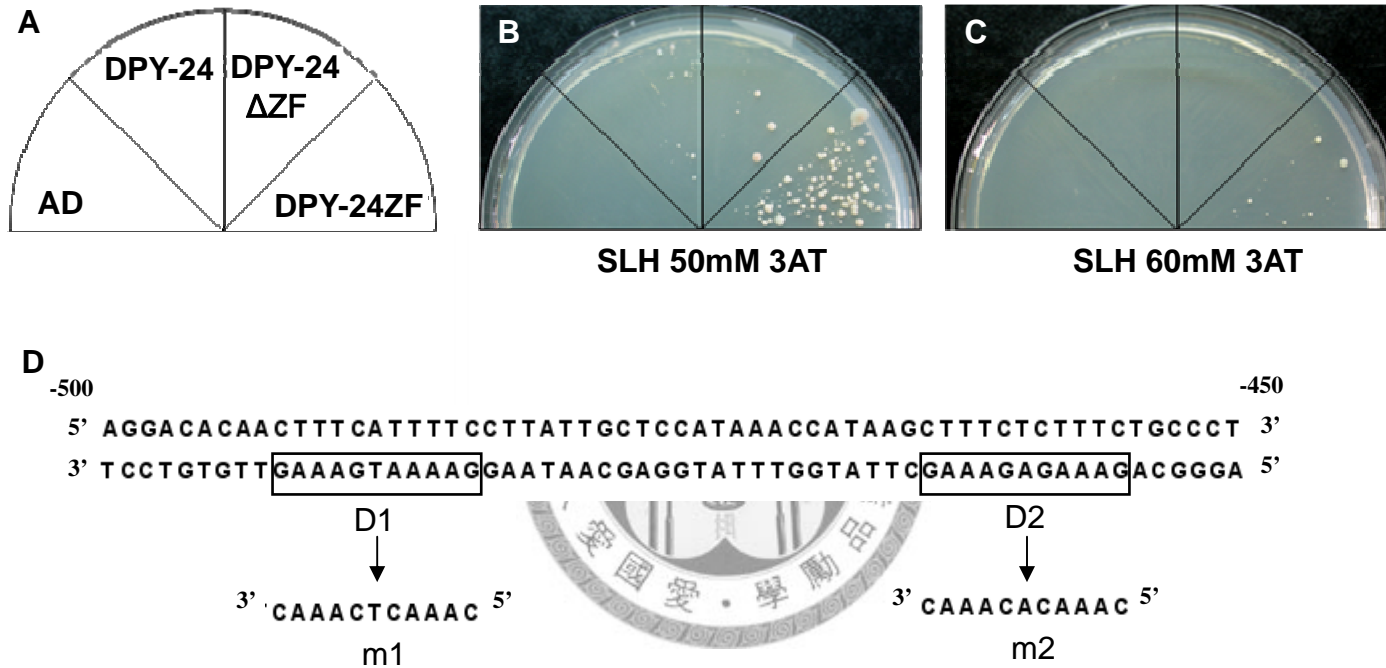


Figure 11. DPY-24 binds to the *unc-5* promoter via its zinc fingers. (A-C) The yeast one-hybrid assay. (A) the diagram indicates the vector (AD) and the tested *dpy-24* fragment; B and C showed the results on SC-Leu-His plates plus 50mM and 60mM 3AT, respectively. (D) The DPY-24 binding sites, D1 and D2, on *unc-5* promoter and the sequence of their mutations, m1 and m2.

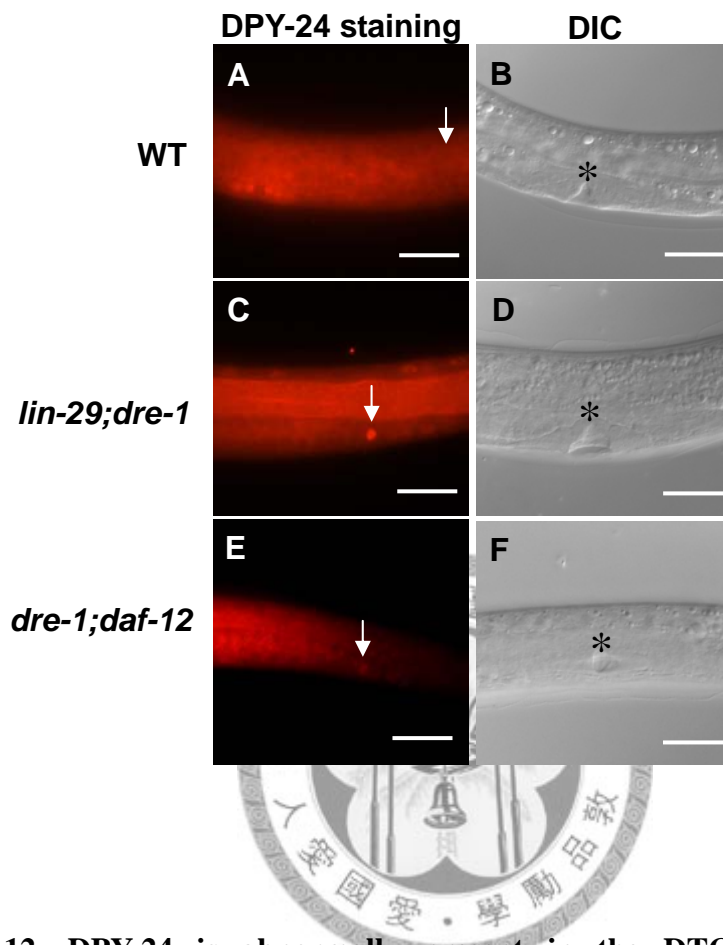


Figure 12. DPY-24 is abnormally present in the DTCs of *lin-29;daf-12*, *lin-29;dre-1* and *dre-1;daf-12* double mutants at the L4 stage.

The wild-type (A), *lin-29;dre-1* (C) and *dre-1;daf-12* (E) L4 worms were stained with anti-DPY-24 antibodies. The right panel (B, D and F) are the Nomarski images of the same worm on the left to confirm the developmental stage. The asterisk and arrow indicate the vulva and DTC, respectively. Scale bars are 20 μ m.

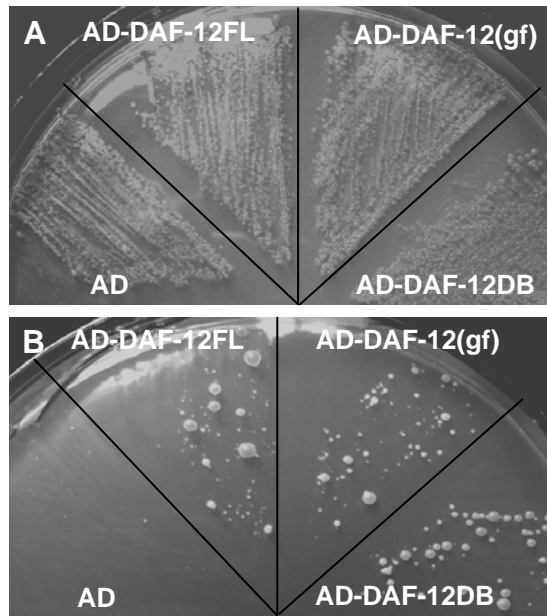


Fig 13. DAF-12 directly binds to the *unc-5* promoter. The yeast one-hybrid assay. A was performed on SC-Leu-His plates while B was on SC-Leu-His plates plus 50mM 3AT.



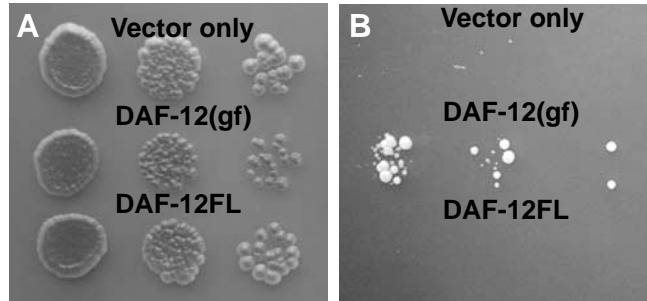


Figure 14. DAF-12 itself could activate the *unc-5* promoter. The yeast transcriptional reporter assay. Each assays was carried out by serial dilution; A was on SC-Trp-Ura-His plate and B was on SC-Trp-Ura-His plate plus 70mM 3AT and 0.05mM CuSO₄.



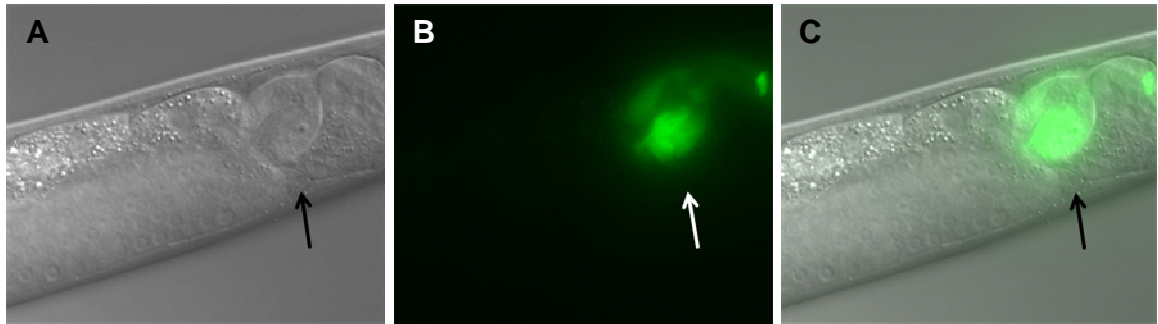


Figure 15. *unc-5* expression is absent in *lin-29;daf-12* double mutant. Images are *lin-29;daf-12* double mutant carrying *Punc-5::gfp* under Nomarski (A) and FITC fluorescence (B) microscopy and (C) is the merge image. Arrows in A indicates the location of DTC and in B indicates the expression of *unc-5* is absent in DTC.



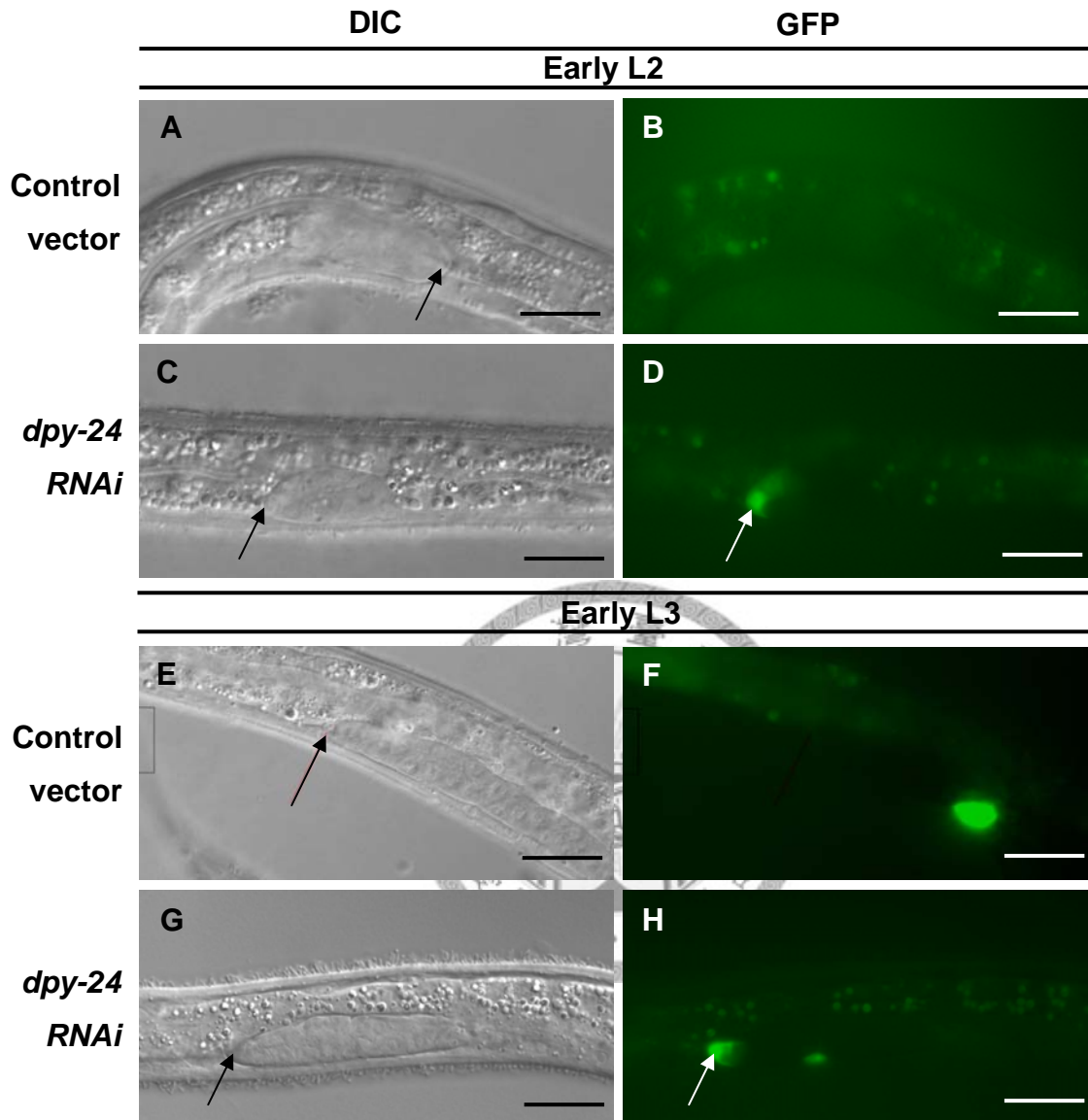


Fig 16. *dpy-24* suppresses the transcription of *lin-29* in early L2. Transgenic animals carrying *P_{lin-29}::gfp* fed with (A,B,E,F) control-vector RNAi and (C,D,G,H) *dpy-24* RNAi. (A-D) are larva at early L2 stage and (E-H) are at early L3 stage. Arrows indicate the location of DTCs. Scale bars are 40 μ m.

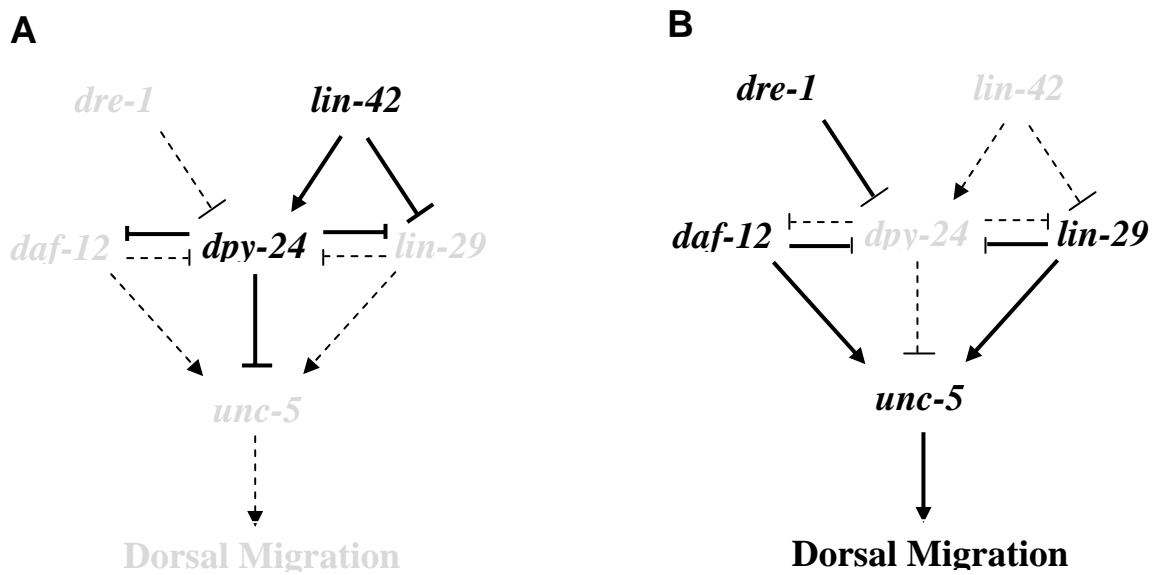


Fig 17. The model of the interaction between *dpy-24* and heterochronic genes to regulate the expression of *unc-5* before mid L3 (A) and during mid L3 (B) when DTCs are about to make their dorsal turn.

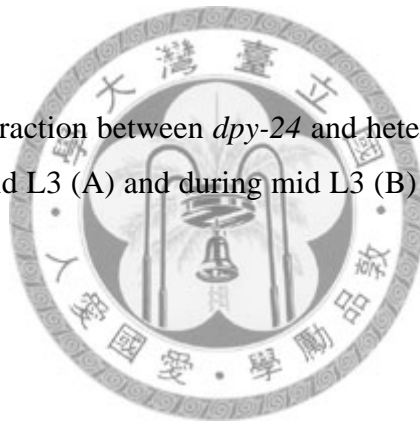
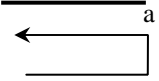
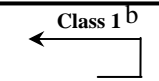
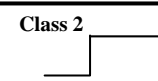
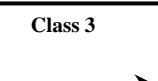


Table 1. DTC migration patterns in *dpy-24* mutants and transgenic worms

Genotype	DTC	WT (%)	defect (%)			Total%
			Class 1 ^b 	Class 2 	Class 3 	
Wild type	A	100	0	0	0	0
	P	100	0	0	0	0
<i>dpy-24(s71)</i>	A	18	24	53	5	82
	P	7	80	13	0	93
<i>dpy-24(tp5)</i>	A	63	12	23	2	37
	P	45	55	0	0	55
<i>dpy-24(tm548)</i>	A	37	33	20	10	63
	P	41	54	5	0	59
<i>dpy-24(tk41)</i>	A	35	43	18	4	65
	P	21	75	4	0	79
<i>P_{lag-2}::unc-5</i>	A	70	14	16	0	30
	P	48	45	7	0	52

a. The graphics indicate the shape of the gonad, *i.e.* the path of DTC migration. The arrow points out the direction and the location of the arrowhead indicates the end. A and P indicate anterior and posterior DTCs, respectively.

b. Class 1 mutants include DTC defects in Figure 1C and 1D.

c. n=50 for each genotype.

Table 2. Genetic interactions of *dpy-24* with *unc-5*, *unc-6*, *unc-40* and *unc-129*.

Genotype	DTC	Precocious				Total% ^c
		←	Dorsal Turn (%)*	← ^a	→ ^b	
<i>dpy-24(s71)</i>	Anterior	18	77	0	5	5
	Posterior	8	92	0	0	0
<i>unc-5(e53)</i>	Anterior	52	0	42	6	48
	Posterior	17	0	81	2	83
<i>dpy-24(s71);unc-5(e53)</i>	Anterior	2	0	0	98	98
	Posterior	2	0	67	31	98
<i>unc-6(rh46)</i>	Anterior	64	0	33	3	36
	Posterior	33	0	67	0	67
<i>dpy-24(s71);unc-6(rh46)</i>	Anterior	2	4	4	90	94
	Posterior	20	6	58	16	74
<i>unc-40(e271)</i>	Anterior	83	0	13	4	17
	Posterior	50	0	50	0	50
<i>dpy-24(s71) unc-40(e271)</i>	Anterior	3	3	3	91	94
	Posterior	8	11	49	32	81
<i>unc-129(ev557)</i>	Anterior	100	0	0	0	0
	Posterior	100	0	0	0	0
<i>dpy-24(s71);unc-129(ev557)</i>	Anterior	21	9	0	70	70
	Posterior	21	48	5	26	31

* Class 1 and 2 defects described in Table 1.

a. DTC has no phase II dorsal migration.

b. DTC migrates towards the end of the body without making dorsal or centripetal turns.

c. Total (%) = a (%) + b (%)

Table 3. The genetic interaction between *dpy-24* and heterochronic genes *lin-29*, *dre-1* and *daf-12* in posterior DTC migration.

	Wild-type (%)	Precocious (%) ^a	Retarded (%) ^b
<i>dpy-24(s71)</i>	7	93	0
<i>lin-29(n543)</i>	100	0	0
<i>dre-1(dh99)</i>	100	0	0
<i>daf-12(rh61rh411)</i>	100	0	0
<i>lin-29(n543);dre-1(dh99)</i>	0	0	100
<i>lin-29(n543);daf-12(rh61rh411)</i>	0	3	97
<i>dre-1(dh99);daf-12(rh61rh411)</i>	0	2	98
<i>dpy-24(RNAi);lin-29(n543);dre-1(dh99)</i>	22	43	35
<i>dpy-24(s71);lin-29(RNAi);daf-12(rh61rh411)</i>	15	37	41
<i>dpy-24(s71);dre-1(dh99);daf-12(rh61rh411)</i>	12	81	7
<i>lin-29(RNAi);dre-1(dh99);daf-12(rh61rh411)</i>	0	0	100
<i>dpy-24(s71);lin-29(RNAi);dre-1(dh99);daf-12(rh61rh411)</i>	17	43	40

^a Percentage of animals with class 1 or 2 defect shown in Figure 1.

^b Percentage of animals in which the DTC delayed phase II dorsal migration.

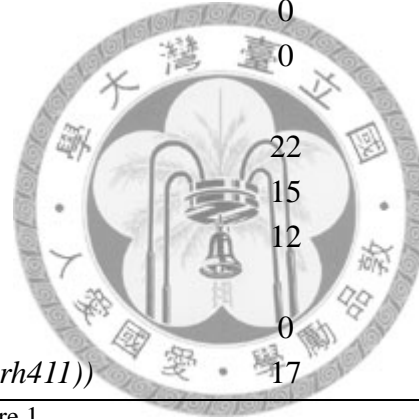


Table 4. Ectopic expression of *lin-29* is sufficient to induce DTC dorsal turn and *unc-5* expression.

<i>Plag-2::lin-29</i>	Precocious dorsal turn (%)	Precocious <i>unc-5</i> expression (%)	n
Line 1	27	14	70
Line 2	9.5	8	84

^a Percentage of animals with class 1 or 2 defect shown in Figure 1.

^b Percentage of animals in which the DTC delayed phase II dorsal migration.

